# Product User Guide & Algorithm Specification

AWI CryoSat-2 Sea Ice Thickness (version 2.4)

Issued by

Alfred Wegener Institute Helmholtz Centre for Polar and Marine Research

Stefan Hendricks

Robert Ricker

Stephan Paul

Date

2021/10/11

**Document Version**

| | | |
|---|---|---|
| Rev 1.0 | 06. May 2019 | Initial Version |
| Rev 1.1 | 27. August 2019 | Update to AWI CryoSat-2 algorithm version 2.2 |
| Rev 1.2 | 23. November 2020 | Update to AWI CryoSat-2 algorithm version 2.3 |
| Rev 1.3 | 11. October 2021 | Update to AWI CryoSat-2 algorithm version 2.4 |

**Table of Contents**

**Parameter & Abbreviation Index**

| | |
|---|---|
| AWI | Alfred Wegener Institute Helmholtz Centre for Polar and Marine Research |
| AMSR2 | Advanced Microwave Scanning Radiometer 2 |
| C3S | Copernicus Climate Change Services |
| CCI | Climate Change Initiative |
| CDR | Climate Data Record |
| CET | Central European Time zone |
| DTU | Danish Technical University |
| EASE | Equal-Area Scalable Earth Grid |
| ELEV | Surface Elevation |
| ESA | European Space Agency |
| FRB | Freeboard |
| FTP | File Transfer Protocol |
| FYI | First-year sea ice |
| GCOS | Global Climate Observing System |
| IUP | Institute for Environmental Physics, University of Bremen |
| LEW | Leading Edge Width |
| LRM | Low Resolution Mode |
| MSS | Mean Sea Surface |
| MYI | Multi-year sea ice |
| NaN | Not a Number |
| NetCDF | Network Common Data Format |
| NRT | near real-time product timeliness |
| OCOG | Offset Centre of Gravity Retracker |
| OSI SAF | Ocean and Sea Ice Satellite Application Facility |
| PP | Pulse Peakiness |
| pysiral | PYthon Sea Ice Radar ALtimetry toolbox |
| REP | reprocessed product timeliness |
| RFRB | Radar Freeboard |
| SAR | synthetic aperture radar |
| SARin | Interferometric synthetic aperture radar |
| SD | Snow Depth |
| SIC | Sea Ice Concentration |
| SIG0 | Nadir Radar Backscatter Coefficient |
| SIRAL | Synthetic Aperture Interferometric Radar Altimeter |
| SIT | Sea Ice Thickness |
| SLA | Sea Level Anomaly |
| SSH | Sea Surface Height |
| TAI | Temps Atomique International |
| TFMRA | Threshold First Maximum Retracker Algorithm |
| TWV | Total number of Waveforms |
| UTC | Coordinated Universal Time |
| VF | Valid Fraction |
| VWF | Number of Valid Waveforms |
| W99 | Warren 99 Snow on Sea Ice Climatology |

# 1   Introduction

## 1.1   Purpose of this Document

This document provides an overview of all aspects of the CryoSat-2 Arctic sea-ice thickness data product (version 2.4) generated at the Alfred Wegener Institute Helmholtz Center for Polar and Marine Research (AWI). It contains information on the

1.  Primary and auxiliary data sets used in the processing
2.  Description of the algorithm used to derive geophysical information along orbit segments and on space-time grids
3.  Technical specifications of the product files
4.  Data access
5.  Known Issues of the data record

## 1.2   Scope of the AWI Sea-Ice Altimetry Production System

The development of a sea-ice (freeboard & thickness) product was started at the Alfred Wegener Institute (AWI) in 2014 with the goal evaluation the mass balance of Arctic sea ice and its uncertainties from CryoSat-2 sea ice altimetry. Since then, the AWI CryoSat-2 sea ice product has been the basis for climate data records (CDR) of European initiatives such as the ESA Climate Change Initiative (CCI) and the Copernicus Climate Change services (C3S) as well as a testbed for algorithm evolutions of these CDR's. It is also an input dataset for the merged CryoSat-2/SMOS sea-ice thickness dataset developed at the AWI. The algorithm development and the resulting data record have contributed to numerous scientific studies and assessments of the state of Arctic sea ice.

The AWI CryoSat-2 product is generated in the Arctic winter month of October through April in near-real time to support operational capability for analyzing the state of Arctic sea ice with minimal time delay.

⚠ An extension of the data product into the southern hemisphere as well as to other satellite altimeters (Sentinel-3A/B, AltiKA, ICESat-2) is under investigation.

## 1.3   Level of Commitment

A central paradigm of the AWI CryoSat-2 sea-ice thickness product is an open science approach with public and open access to data products and the underlying software. The development target is to support the FAIR principles[1] for data science.

Our intention is to develop and implement algorithm evolutions on a yearly basis. The update of the production system will occur during the summer period, when no sea-ice thickness data is available. The entire CryoSat-2 time series will be reprocessed with the new algorithm to have a consistent sea ice data record and the processing will resume with the new product version in October.

We are firmly committed to maintain and update the AWI sea ice altimetry production system for the near future, though no direct external funding exists for this activity.

---

[1] https://www.go-fair.org/fair-principles/

## 1.4    Target Requirements

The target requirements for sea ice thickness in terms of uncertainty and stability of a data record for climate research have been defined in the most recent GCOS document (GCOS report no. 154: SYSTEMATIC OBSERVATION REQUIREMENTS FOR SATELLITE-BASED DATA PRODUCTS FOR CLIMATE, 2011 update. Supplemental details to the satellite-based component of the "Implementation Plan for the Global Observing System for Climate in Support of the UNFCCC (2010 Update)" December 2011, ref. 18).

Table 1: GCOS Target requirements and achievable performance [D3] for remote-sensed sea ice thickness product in climate applications

| Requirement | GCOS Target | Achievable Performance |
|---|---|---|
| Horizontal Resolution | 25 km | 25 km |
| Temporal Resolution | Monthly | Monthly |
| Accuracy | 0.1 m | 0.5 m |
| Stability | Unspecified | Unspecified |

While the sea ice thickness product meets the GCOS target requirements for horizontal and temporal resolution, the expected product uncertainty is larger than the GCOS requirement of 10 cm. No specification is given for the stability of the sea ice thickness time series.

## 1.5    Further Information

### 1.5.1    CryoSat-2 Input Data

For all information of the CryoSat-2 mission and ESA data products please refer to the *CryoSat Product Handbook*, which is available for download at the ESA Earthnet Online. Additional information on the status of CryoSat-2 and its data products can be found on the following websites:

ESA – Living Planet Programme – CryoSat

ESA – CryoSat-2 Wiki

UCL - CryoSat Performance and Quality Monitoring

### 1.5.2    AWI Online Documentation and Blog

News and updates of the AWI CryoSat-2 sea ice product can be found online

AWI – Sea Ice Radar Altimetry Wiki

AWI – Sea Ice Radar Altimetry Blog

## 2    Production System

This section describes the production system, which consists of the software environment, its configuration, and the input datasets.

### 2.1    Processing Environment

The processing system is based on pysiral, the python sea ice radar altimetry toolbox. The toolbox is developed as an open-source project (https://github.com/shendric/pysiral). The software package and all management scripts are under revision control and run in a CentOS based environment. Version 2.4 of the AWI CryoSat-2 sea ice product is generated with the ⅄`production/awi-v2p4` branch of the git repository.

### 2.2    Product Timeliness

Sea ice products are generated at two timeliness versions based on the two data streams of input data from CryoSat-2:

| | |
|---|---|
| NRT (near-real time) | + 2 days |
| REP (reprocessed) | + 33 days |

Processing at AWI infrastructure is scheduled at early morning CET, which adds a few hours to the timeliness after the availability of input data at ESA servers.

NRT products are obsolete when a REP product is available for the same period.

### 2.3    Input Data

Input data falls in two categories: 1) primary data consisting of radar altimeter data over ice-covered ocean and 2) auxiliary data as data sets that are used for the parametrization of the sea-ice thickness retrieval algorithm.

#### 2.3.1    Primary Altimeter Data

The primary radar altimeter dataset for the AWI sea ice product is the CryoSat-2 Level-1B data record from the ESA instrument processing facility. The product files contain geolocated echo waveforms, range corrections and flags of the radar altimeter SIRAL. The altimeter data covers a narrow swath along the nadir point of the satellite orbits.

The altimeter operates in different modes[2] depending on surface type. Sea ice areas are covered by SAR and SARin modes and data from both modes are utilized in the AWI sea ice processor.

⚠ Version 2.4 of the AWI CryoSat-2 sea ice product is based on two different versions of the CryoSat-2 L1B data: Baseline-D from 2010/11 – 2021-04 and Baseline-E from 2021/10 and later.

---

[2] https://earth.esa.int/web/guest/-/geographical-mode-mask-7107

Table 2: CryoSat-2 orbit and radar altimeter parameters

| Data Period | Northern winter month (full) | Nov 2010 – on-going |
|---|---|---|
| **Orbit** | Repeat cycle | 369 days; 30-day sub-cycle |
| | Altitude | 717 km |
| | Inclination | 92.00° |
| | Period | 100 minutes |
| **Radar Altimeter** | Name | SIRAL |
| | Wave band | 13.575 GHz (Ku-Band) |
| | Type | Doppler-delay (SAR)<br>Doppler-delay interferometric (SARin) |
| | Footprint | 0.3 km x 1.6 km (along x across track) |

2.3.2    Auxiliary Parameter

Datasets that provide auxiliary parameters to the geophysical retrieval are listed below in Table 3. Since algorithm version 2.2, the source of auxiliary data depends on the timeliness (see 2.2), with operational sea ice concentration and type for the CryoSat-2 near-real time product and the sea ice concentration and type (interim) climate data record from the Copernicus Climate Change Services (C3s) for the reprocessed sea ice thickness product.

Table 3: Auxiliary sea ice parameter and their sources

| Parameter | Description | Temporal Resolution | Source |
|---|---|---|---|
| Mean Sea Surface Height | DTU21: Gridded mean sea surface height from multi-sensor altimetry data | Static | DTU Space (FTP) |
| Sea Ice Concentration NRT | Daily Sea Ice Concentration Analysis from OSI SAF EUMETSAT (OSI-401-b) | Daily | EUMETSAT OSISAF (http://www.osi-saf.org/) |
| Sea Ice Concentration REP | OSI-SAF Sea Ice Concentration (Interim) Climate Data Record (CDR/ICDR) | Daily | C3S Climate Data Store (Link) |
| Sea Ice Type NRT | Daily Sea Ice Type Analysis from OSI SAF EUMETSAT (OSI-403-d) | Daily | EUMETSAT OSISAF (http://www.osi-saf.org/) |
| Sea Ice Type REP | Sea Ice Type (Interim) Climate Data Record (CDR/ICDR) | Daily | C3S Climate Data Store (Link) |
| Snow depth on sea ice | Merged Climatology from IUP AMSR2-based snow depth and Warren Climatology | Monthly (Static) | (see section 4.4) (FTP) |

### 2.3.3    Sea-ice Type optimizations

The sea-ice type (i)cdr data does not provide information close to the coast. Since the estimation of snow depth and sea-ice density requires the sea-ice type input, a gap in the sea-ice type information results in a data gap of sea-ice freeboard and thickness.

In version 2.3, a gap-filling method was introduced to the sea-ice type data class with the purpose to improve the data availability close to the coast, especially within the Canadian Archipelago. The gap filling method is based on the following conditions:

Table 4: Conditions for gap-filling of sea-ice type (i)cdr based on the sea-ice concentration auxiliary data

| Sea Ice Type | Sea Ice Concentration | Action |
|---|---|---|
| Sea ice type is "no data" and nearest valid information exist within 45 km | Sea-ice concentration > 70% | sea ice type value set to nearest neighbor |
| Sea ice type is "no data" and nearest valid information exisit within 45 km | Sea-ice concentration > 70% | sea ice type value set to ambiguous (multi-year ice fraction 0.5) |
| Sea ice type is invalid | Sea-ice concentration < 70% | Sea-ice type remains "no data" |

## 2.4   Processing Levels

The production system yields a series of data products that build on each other. For the naming of these processing levels, we adopt the following naming convention[3]:

Table 5: Definition of data processing levels

| Level | Code | Description |
|-------|------|-------------|
| Level 0 | L0 | Sensor raw data (not used here) |
| Level 1 | L1A | L0 data with ancillary data (not used here) |
| | L1B | Calibrated L1A data at full sensor resolution |
| | L1P | Processed L1B data (e.g., remapping of coverage) |
| Level 2 | L2 | Geophysical variables at the same resolution and location as L1B/L1P data |
| | L2i | L2 data with flags and auxiliary data |
| | L2P | Post-processed L2i data |
| Level 3 | L3 | L2 data mapped on a space-time grid |
| | L3C | Observations combined from a single instrument into a space-time grid. |
| | L3S | Observations combined from multiple instruments into a space-time grid. |
| Level 4 | L4 | Data sets created from the analysis of lower-level data that result in gridded, gap-free products. |

---

[3] Adapted from CCI Data Standards v2, ESA Document CCI-PRGM-EOPS-TN-13-0009

## 2.5   Processing Workflow

The process to derive higher level (L2, L3) data products from the input (L1) data products is handled by a set of dedicated and self-contained software elements. These are specified in Table 6 and Figure 1. Their content is described in detail in the following sections.

Table 6: Overview of dedicated processors in the sea ice production system

| Level | Description | Input | Output |
|---|---|---|---|
| Level-1 Pre-Processor | Prepares and harmonizes the L1 input data | L1B | L1P |
| Level 2 Processor | Retrieval of geophysical parameters (freeboard and thickness) | L1P | L2i |
| Level 2 PreProcessor | Daily summaries of geophysical data at full resolution (trajectory data) | L2i | L2P |
| Level 3 Processor | Gridded data over weekly or monthly periods (space-time grids) | L2i | L3C |
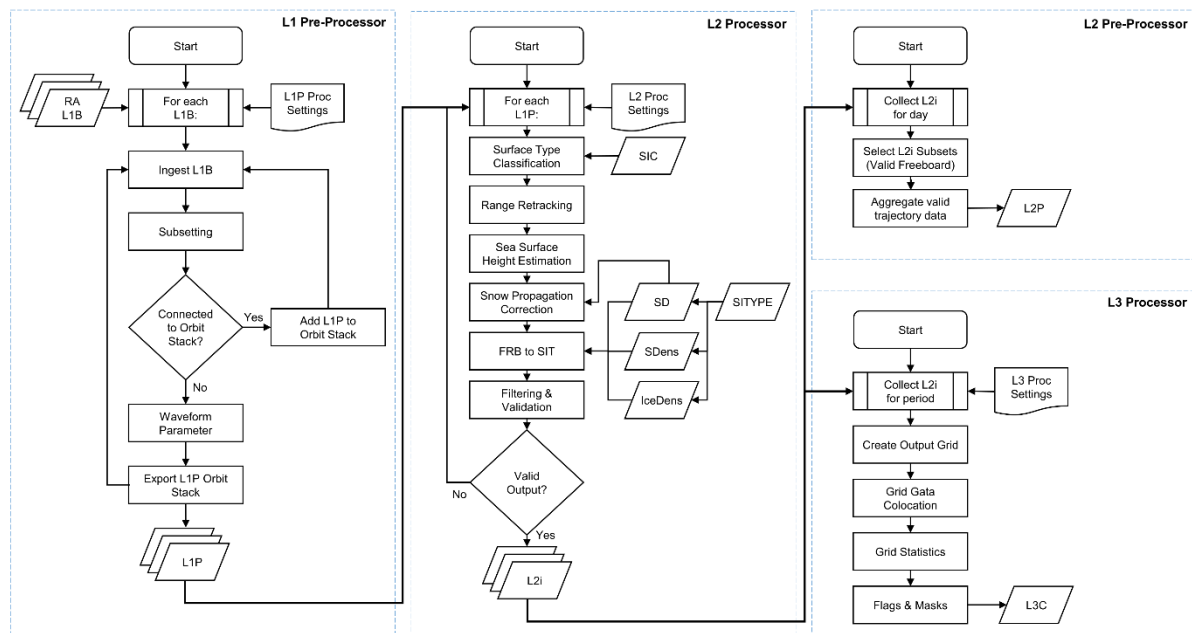


Figure 1: Workflow of the sea ice production system

## 2.6    Version History

This document and its updates always refer to the latest version of the production system and retrieval algorithm at the time of publication. This section provides lists of changes between two consecutive versions.

### 2.6.1     Fall 2021 Update (v2.4)

*Input Data*

- CryoSat-2 ICE baseline E data as primary altimeter data now used for the operational near real-time and reprocessed data generation from October 2021 and later. The previous data record (Nov 2010 till April 2021) is based on the previous L1B version (ICE baseline D).

*Auxiliary Data*

- Updated C3S sea ice type (interim) climate data record from version 1 to version 2 (reprocessed data only).
- Updated OSI-SAF operational sea ice type to version OSI-403-d.
- Updated mean sea surface from DTU15 to DTU21.

Algorithm

- Surface type classification: Sea ice mask is now based on 15% sea ice concentration threshold. The threshold was 70% in previous versions.
- Used `uncertainty´ field in OSI-403-d sea ice type files instead of parametrization based on `confidence` flags of previous versions.
- The sea ice thickness quality flag is no longer automatically set to 'intermediate' outside the central Arctic basin.

Product format and content

- Flag values of the status flag (l3c variable `status_flag`) have been changed. Flag value 0 is now `nominal` and other values have been shifted accordingly.
- Flag values of the quality flag (l3c variable `quality_flag`) have been changed. Flag value 0 is now `nominal` and the 'no data' has been moved to flag value 3.
- Various changes to the global and variable attributes to improve compliance with newer versions of the Climate & Forecast (CF) and Attribute Convention for Dataset Discovery (ACDD) standards.

Level-1 Pre-Processor

- Added L1 preprocessor for CryoSat-2 L1b for ICE baseline-E.

### 2.6.2     Fall 2020 Update (v2.3)

*Input Data*

- CryoSat-2 baseline-D data as primary altimeter data now used for the full reprocessed data record since November 2010.

*Auxiliary Data*

- Switched C3S sea-ice concentration (interim) climate data record from v1.2 to v2.0
- Reverted mean sea surface from DTU18 to DTU15
- Optimized sea-ice type information near coasts and in the Canadian Archipelago

Algorithm

- Updated computation of wave speed correction in the snow layer following Mallett et al., 2020
- Used hemisphere-wide snow density values following Mallett et al., 2020
- Snow depth and density values are updated daily instead of monthly to avoid freeboard and thickness discontinuities at a change of month
- Optimizations in the estimation of along-track sea-level anomaly

Product format and content

- Field sea level anomaly is now named ´sea_level_anomaly´ instead of ´sea_surface_height_anomaly´

Level-1 Pre-Processor

- Fixed an issue that resulted in loss of data for the SARin radar mode (most severe in the Canadian Archipelago). Data was rejected based on an incorrect interpretation of the measurement confidence flag for baseline-D SARin data files.

### 2.6.3 Fall 2019 Update (v2.2)

*Input Data*

- CryoSat-2 baseline-D data as primary altimeter data since April 28, 2019. NOTE: In v2.2 the reprocessed grid products consist of a mix between baseline-C and baseline-D

*Auxiliary Data*

- Use C3S (interim) climate data records of sea ice concentration as auxiliary data for the reprocessed data stream. This fixes an issue with evolving land masks in the OSI-SAF operational products, which will not be reprocessed to a consistent standard. The C3S sea ice type is also known to be more precise in the marginal ice zone

*Level-1 Pre-Processor*

- Added support for the new ESA baseline-D netCDF format
- Increased the regional subset from 50N – 88N in version 2.1 to 45N – 88N

*Level-2 Processor*

- Split algorithm between near-real time and reprocessed with timeliness dependent choice of validation data
- Removed requirement of having a minimum of 3 leads in each orbit.
- Added sea ice draft and sea ice draft uncertainty as output variables
- Renamed freeboard to sea ice freeboard to be in line with the variables standard name

*Level-3 Processor*

- Added sea ice draft and sea ice draft uncertainty as output variables
- Renamed freeboard to sea ice freeboard to be in line with the variables standard name
- Removed the average Level-2 orbit-based uncertainty for radar freeboard, sea-ice freeboard and sea-ice thickness
- All statistical variables are now named with a "`stat_`" prefix in the variable name for clarity
- Added temporal statistics variables (see Temporal Coverage per grid cell6.5.2)
- Added the fraction of negative thicknesses per grid cell as statistical parameter
- Added geotiff output (variable sea-ice thickness only) for all gridded products

# 3  Preparation of Primary Altimeter Data (Level-1 Pre-Processor)

The main purpose of the Level-1 Pre-Processor is to select appropriate subsets along the orbit of the satellite for the retrieval of sea ice parameters. The production system has also been designed to process data from other radar altimeter satellites then CryoSat-2, therefore one task is the generation of a unified L1P data format for generating higher level sea ice products.

The steps specific for CryoSat-2 are described below.

## 3.1  File format conversion

CryoSat-2 Level-1b data is delivered by ESA in form of a custom data format for ESA Earth Observation data. The variables in these files are converted to SI units and the timestamp is converted from TAI to UTC. Variables that are only available in 1Hz are interpolated to the 20Hz of the waveform data.

After the merging of relevant orbit segments (see section below), the data is saved in a NetCDF format following the pysiral L1P conventions. The content of the L1P files are several data groups:

1. Metadata
2. Time-orbit data (location and orientation of the satellite)
3. Radar waveforms
4. Geophysical range corrections
5. Surface type information
6. Waveform Classifiers

## 3.2  Subsetting and merging of orbit segments

A specific characteristic of CryoSat-2 radar altimeter data is the division of orbit segments in the three different radar modes (LRM, SAR & SARin). Data from these modes are disseminated in separate product files and the pre-processor merges of individual segments where appropriate. For this purpose, the L1B input files are organized as a stack of orbit segments and processed sequentially. The rationale for the merging is to enable sea-surface height estimation for a full crossing of the Arctic basin. A practical example is shown in Figure 2.

### 3.2.1  Orbit Subsetting

We use a southern latitude threshold of 50N as an initial regional limitation for the Arctic sea ice domain.

### 3.2.2  Orbit Segment Merging

Within the Arctic domain, consecutive CryoSat-2 L1B files are considered as connected when the difference between the last timestamp of the first and the earliest timestamp of the second orbit segment is not larger than 10 seconds.

Before the merging, the range window of SARin data is reduced to 256 range bins to allow merging with SAR orbit segments.
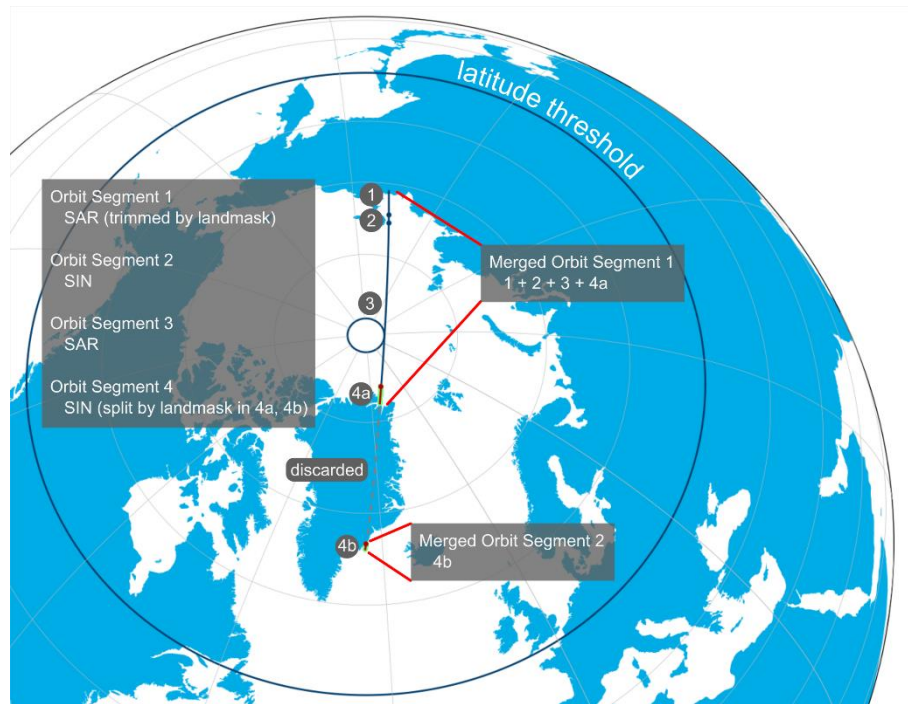
Figure 2: Exemplary merging of connected CryoSat-2 L1B product files with different radar mode by the Level-1 pre-processor

### 3.2.3    Data over land

Data over land or other non-ocean surface types are identified with the surface type flag in the CryoSat-2 L1B data products. Such segments are trimmed from if they occur at the edges of merged segment. If these are embedded in ocean data to both sides, they can remain if it does not affect more than 1000 data points the 20Hz samples (~ 300 km). Larger non-ocean segments are discarded, and the orbit segmented is separated into two unconnected parts.

## 3.3    Computations of Waveform Classifiers

The Pre-processor also computes several waveform shape parameters and stores them in the L1P files for later use in the Level-2 Processor. A list of these parameters is given below:

1. Radar backscatter coefficient $\sigma_0$ in dB
2. Pulse peakiness, left & right peakiness according to Ricker et al., 2014
3. OCOG parameters (width & amplitude)
4. Leading edge width (defined as the distance between 5% to 95% TFMRA), as well as the width of the first and second half of the leading edge (50% TFMRA)

# 4    Geophysical Retrieval Algorithm (Level-2 Processor)

The AWI sea-ice Level-2 processor consists of two major steps:

1. Estimation of sea-ice freeboard from CryoSat-2 radar waveforms
2. The conversion of sea-ice freeboard into sea-ice thickness with auxiliary datasets
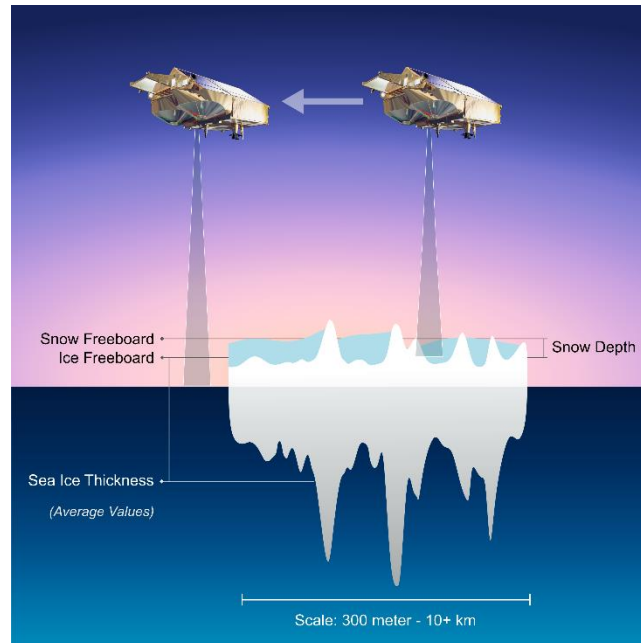


Figure 3: Principle of sea ice thickness retrieval with radar altimetry: Freeboard is derived as differential range measurements over sea ice and open water surfaces and converted into sea ice thickness based on the Archimedes Principle.

The first step requires the processing of all available CryoSat-2 Level-1b data over Arctic sea ice, while the second step consists of the interpretation of the retrieved freeboard values. Both steps require assumptions and simplifications, which are based on results of validation activities by ESA and partner organizations. These are described in the following sections. It is a major goal of this processor to estimate not only sea-ice thickness, but also the quantification of uncertainties, which arise from of the quality of the level-1b and the necessary assumptions and simplifications.

## 4.1    Surface Type Classification

Fundamental to freeboard retrieval is the classification of surface types for each radar echo. We consider three different surface types:

1. ice surface used for freeboard and thickness retrieval
2. lead/opening between ice floes used for sea surface height estimation
3. mixed surface/unknown that are discarded from further processing

The classification is based on three parameter that describe the waveform shape and have distinct properties for waveforms over leads and ice surfaces:

1. radar backscatter coefficient (SIG0)
2. pulse peakiness (PP)
3. leading edge width (LEW)

The radar backscatter coefficient describes the reflectivity of the surface and is strongly related to the maximum power of the waveform. The pulse peakiness follows the definition of Ricker et al. (2014):

$$PP = \sum_{i=1}^{N_{wf}} \frac{\max{(WF)}}{WF_i} \cdot N_{wf}$$

The leading-edge width is defined as the width in range bins along the power rise to the first maximum between 5 % and 95 % of the first-maximum peak power while using a ten-time oversampled waveform.

Thresholds for each of the three parameters have been defined for each month and each radar mode as SARin waveforms have different properties than SAR waveforms. In addition, only areas with sea ice concentrations (SIC) greater than 70% are considered a valid area for detection of leads and sea ice. The thresholds originate from Paul et al., 2018 and are summarized in tables 4 and 5.

Table 7: Waveform classification thresholds for surface type: lead

| Metric | Month | CryoSat-2 SAR | | CryoSat-2 SARin | |
|--------|-------|------|------|------|------|
| | | Min | Max | Min | Max |
| PP | JAN | 67.30 | | 264.30 | |
| | FEB | 66.30 | | 257.90 | |
| | MAR | 66.60 | | 253.60 | |
| | APR | 69.90 | | 264.60 | |
| | OCT | 76.00 | | 291.80 | |
| | NOV | 73.80 | | 288.80 | |
| | DEC | 68.60 | | 272.60 | |
| SIG0 | JAN | 23.80 | | 24.90 | |
| | FEB | 23.20 | | 25.00 | |
| | MAR | 23.30 | | 24.10 | |
| | APR | 23.40 | | 24.50 | |
| | OCT | 28.00 | | 29.00 | |
| | NOV | 25.80 | | 27.40 | |
| | DEC | 24.10 | | 25.80 | |
| LEW | JAN | | 0.77 | | 1.10 |
| | FEB | | 0.78 | | 1.11 |
| | MAR | | 0.78 | | 1.13 |
| | APR | | 0.76 | | 1.09 |
| | OCT | | 0.72 | | 1.02 |
| | NOV | | 0.73 | | 1.03 |
| | DEC | | 0.76 | | 1.07 |
| SIC | All | 15 | | 15 | |

Table 8: Waveform classification thresholds for surface type: sea ice

| Metric | Month | CryoSat-2 SAR | | CryoSat-2 SIN | |
|---|---|---|---|---|---|
| | | Min | Max | Min | Max |
| PP | JAN | | 30.50 | | 99.40 |
| | FEB | | 28.70 | | 94.20 |
| | MAR | | 28.10 | | 89.90 |
| | APR | | 28.50 | | 90.00 |
| | OCT | | 35.40 | | 114.40 |
| | NOV | | 34.90 | | 113.90 |
| | DEC | | 31.90 | | 103.80 |
| SIG0 | JAN | 2.5 | 20.80 | 2.5 | 21.40 |
| | FEB | 2.5 | 19.90 | 2.5 | 20.90 |
| | MAR | 2.5 | 19.60 | 2.5 | 20.10 |
| | APR | 2.5 | 19.00 | 2.5 | 19.10 |
| | OCT | 2.5 | 25.70 | 2.5 | 24.30 |
| | NOV | 2.5 | 23.20 | 2.5 | 23.70 |
| | DEC | 2.5 | 21.10 | 2.5 | 22.00 |
| LEW | JAN | 1.02 | | | 1.55 |
| | FEB | 1.08 | | | 1.58 |
| | MAR | 1.10 | | | 1.62 |
| | APR | 1.11 | | | 1.64 |
| | OCT | 0.91 | | | 1.44 |
| | NOV | 0.90 | | | 1.44 |
| | DEC | 0.97 | | | 1.51 |
| SIC | All | 15 | | 15 | |

## 4.2   Surface Elevation

We use an implementation of the Threshold First Maximum Retracker Algorithm (TFMRA, Ricker et al, 2014) to estimate the range to the main scattering horizon for each waveform. The sub-waveform retracker estimates the range by computing the time where the power of the smoothed leading edge has risen to a defined percentage (Table 9) of the peak power value (see Figure 4).

Table 9: Retracker threshold parametrization for radar range retrieval over lead and ice surfaces

| | Lead Waveforms | Sea Ice Waveforms |
|---|---|---|
| CryoSat (SAR/SIN) | 50% | 50% |
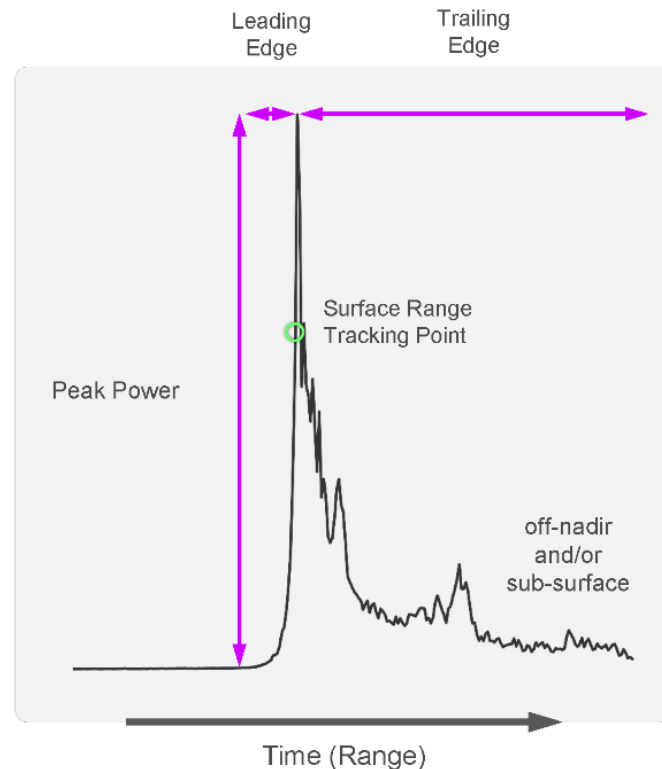
Figure 4: Example of a radar echo power as function of time with waveform shape parameters and tracking point.

The TFMRA returns a time that is converted into range by assuming vacuum light speed as wave propagation velocity. The actual wave propagation speed varies with the properties of the ionosphere and troposphere and the following corrections supplied by the primary data products are added to the range estimate:

- Ionosphere correction
- Dry troposphere correction
- Wet troposphere correction

In addition to atmospheric corrections, the range is corrected to account for sea level changes due to tides and atmospheric pressure:

- Inverse barometric correction
- Elastic ocean tide
- Long-period ocean tide
- Ocean loading tide
- Solid earth tide
- Geocentric polar tide

The source for the geophysical range corrections are CryoSat-2 L1b product finals. The final step is then the computation of surface elevation relative to the WGS84 ellipsoid by subtracting the retrieved range from the altitude of the satellite.

The uncertainty for the range retrieval and the surface elevation based on the noise of the waveform is parametrized as fixed values: 10cm.

## 4.3 Sea surface height

The estimation of the instantaneous sea surface height SSH along the trajectory is computed in steps:

1. Elimination of major sea level changes caused by geoid and mean dynamic topography by subtracting a mean sea surface elevation (DTU21, see 2.3.2)
2. Smoothed interpolation between elevation tie points in leads and extrapolation to the full trajectory (sea level anomaly, SLA)
3. Uncertainty computation and filtering of SLA based on total number and distance to the next SSH tie point.

Generally written SSH is defined as:

$$ssh = mss + sla$$

The uncertainty of the sea surface height depends on the base SSH uncertainty and the distance to the closest sea surface height tie point. The values for base SSH uncertainty is assumed to be 2 cm to include effects such as leads covered with thin ice and the maximum uncertainty is assumed as 10 cm based on investigations of the typical variation of the anomaly between the instantaneous sea surface height and mean sea surface along polar crossing orbits.

The sea surface height uncertainty is computed as

$$\sigma_{SSH} = \begin{cases} 0.02m + 0.1m \times \left( {d_{tp}}/{100km} \right)^2, & d_{tp} < 100km \\ 0.1m, & d_{tp} \geq 100\ km \end{cases}$$

With $d_{tp}$ as the distance to the next sea surface height tie point.

## 4.4 Snow on sea ice

The sea-ice thickness retrieval from altimeter data critically depends on the knowledge of snow (depth and density) information. In absence of a basin-scale observational data set, we utilize climatological information from the Warren et al. 1999 (W99) snow climatology of Arctic sea ice. The W99 climatology is presented as a two-dimensional quadratic fit valid for the central Arctic Basin. Earlier versions of the AWI CryoSat-2 sea ice product used W99 snow information for the ice-covered oceans in the northern hemisphere with the result of data gaps where the quadratic fit resulted in unrealistic or unphysical snow depth and density values.

### 4.4.1 Snow Depth

With version 2.1 we introduced a monthly snow depth and density parametrization based on merging of the W99 snow climatology and daily snow depth over first-year sea ice from AMSR2 data provided by the Institute for Environmental Physics of the University Bremen (IUP).

To merge the two data sets, we create a monthly composite of the IUP AMSR2 snow depth fields to match the monthly resolution of the W99 climatology for the month of October through April. Then we low pass filter the IUP AMSR2 snow depth composite with a Gaussian filter with the size of 8 grid cells, remove negative snow depth values and limit the upper range to 60 cm. Finally, we create a regional weight factor $w$ that ensures a smooth transition between the inner Arctic Basin domain and the area where the AMSR2 data is used. The merged snow depth $sd_{merged}$ is computed as:

$$sd_{merged} = w \cdot sd_{W99} + (1 - w) \cdot sd_{AMSR2}$$

See Figure 6 for visual examples of the merging steps and Figure 6 for the regional weight factor.

The uncertainty of the merged snow depth is derived in a similar fashion. We merge the uncertainty provided by the W99 climatology and the IUP AMSR2 snow depth using the regional weighting factor.

$$\sigma_{sd}^{merged} = w \cdot \sigma_{sd}^{W99} + (1 - w) \cdot \sigma_{sd}^{AMSR2}$$

It is common practice to modify the W99 snow climatology by reducing its value by 50% over first-year sea ice in the central Arctic and we maintain this practice in the Level-2 processing with the ice type information for the orbit. However, the scaling should not be applied on the AMSR2 snow depth and use the following approach to only scale the snow depth contribution from the W99 climatology. The snow depth $sd$ is thus

$$c = (1 - f_{myi}) * c_{fyi} * w$$
$$sd = sd_{merged} - c \cdot sd_{merged}$$

where $c_{fyi} = 0.5$ is the W99 scaling for first-year sea ice, $c$ the total scaling factor that includes the multi-year sea ice fraction $f_{myi}$ and the weight factor. The uncertainty of $sd$ is represented as the scaled uncertainty plus an uncertainty term for the scaling itself

$$\sigma_{sd} = \left( \sigma_{sd}^{merged} - c \cdot \sigma_{sd}^{merged} \right) + \left( sd \cdot c \cdot \sigma_{f_{fyi}} \cdot c_{fyi} \right)$$

The result of the merging process is significantly less data gaps outside the central Arctic Basin (see Figure 7), while the retaining the W99 information in areas potentially covered with multi-year sea ice, where AMSR2 lacks sensitivity.

Utilization of the monthly fields leads to unrealistic jumps in daily (l2p) sea-ice freeboard and thickness values between the last day of a month and the first day of the next. From version 2.3 on, the monthly climatology is attributed to a reference day and linear interpolation is used between these days.

The reference day for the monthly climatology is the center of the month except for October and April. The reference day for these months is set to be the beginning and end respectively, as the merged snow climatology does not exist for September and May and extrapolation prove unreliable.

Table 10: Reference dates for the monthly snow climatology used for the estimation of linear interpolated snow depth with daily resolution

| Month | October | November | December | January | February | March | April |
|---|---|---|---|---|---|---|---|
| Reference Day | 1.10. | 15.11. | 15.12. | 15.1. | 15.2 | 15.3 | 30.3 |

The linear interpolation only affects the snow depth values before the ice-type based 50% correction.
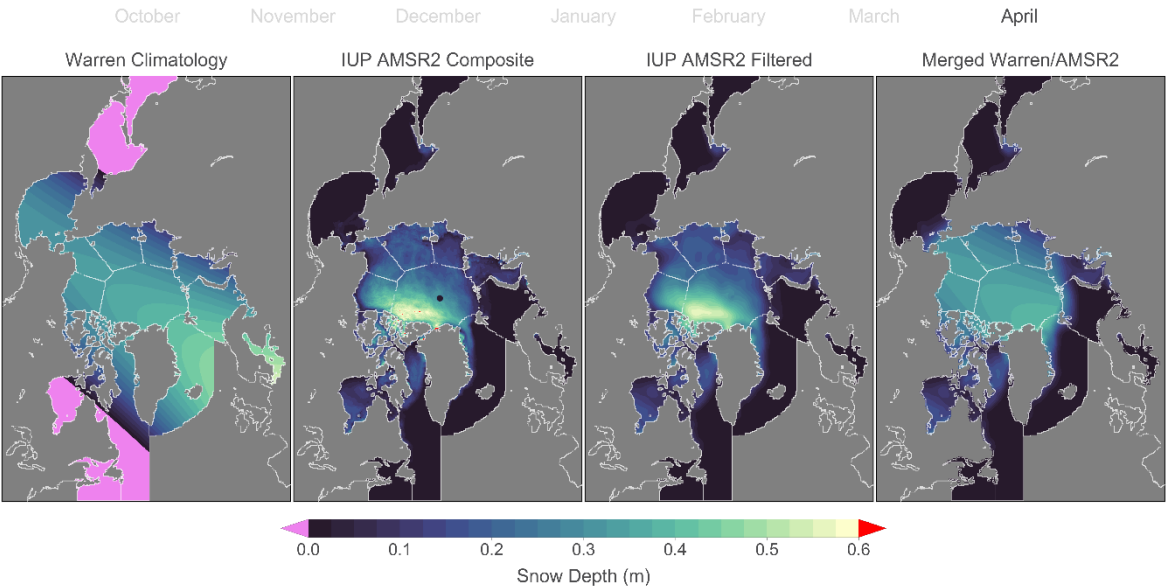
Figure 6: Steps to create a monthly merged snow depth climatology from the Warren snow climatology and monthly composites of snow depth fields derived from AMSR2 brightness temperatures by IUP Bremen. Example April, from left to right: 1) Warren snow climatology, 2) Monthly IUP snow composite from daily data, 3) Low-pass filtered IUP data and 4) merged Warren/AMSRE2 with regional weighting factor.
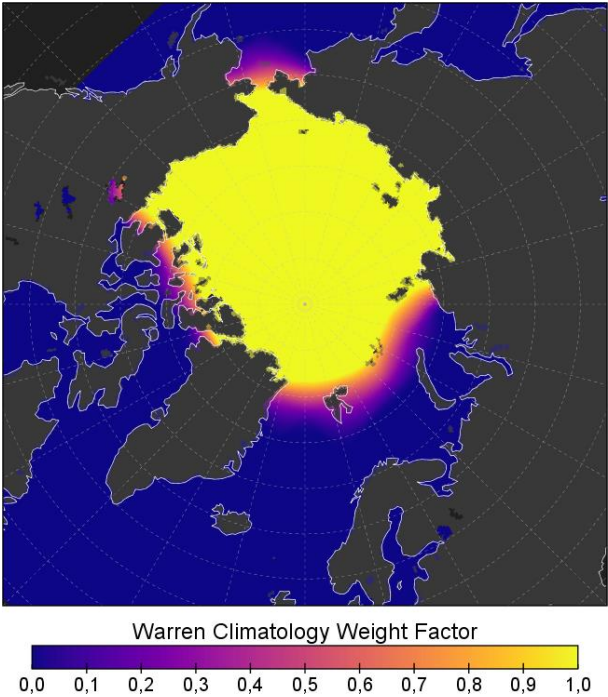


Figure 6: Regional weight factor for the Warren snow depth climatology of Arctic sea ice
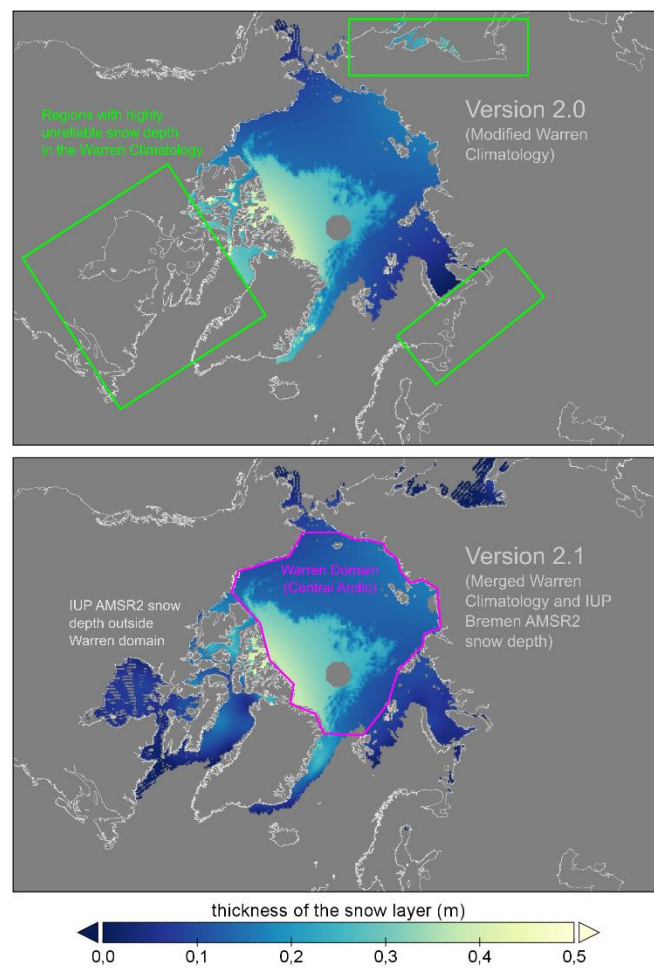
Figure 7: Comparison of W99 only (upper panel) used in v2.0 of the AWI CryoSat-2 sea ice product and merged W99 snow depth climatology (lower panel) modified by sea ice type introduced in v2.1. The merged Warren/AMSR2 snow depth climatology improves the snow depth information in areas outside the domain of the W99 climatology (central Arctic Basin)

### 4.4.2    Snow Density

For version 2.3 we use a linear increasing snow depth over the winter season following Mallett et al., 2020. This replaces using the average of snow density in the central Arctic Basin in version 2.2. The difference between the two solutions is shown in Figure 8. Similar to snow depth, the increase of snow density is computed with daily resolution.

$$\rho_s = 6.5 \ \times t + 274.51$$

With $t$ representing the time in fractional month since October 15.
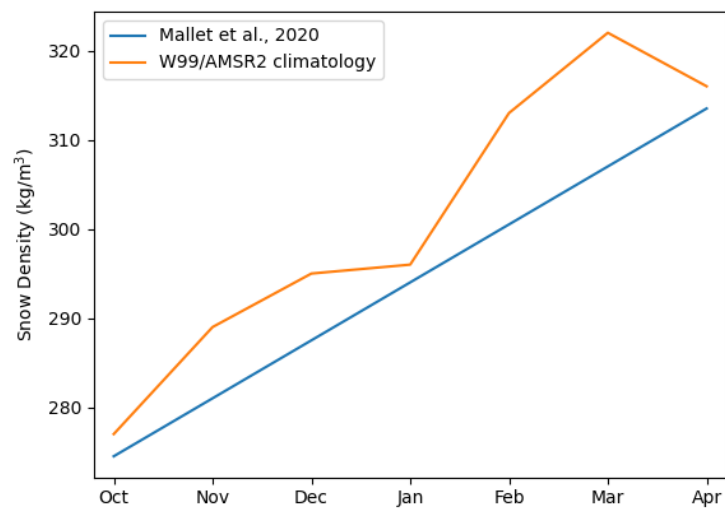
Figure 8: Difference of snow density based on the average in the Arctic Basin (W99/AMSR2 climatology; version 2.2) and the linear increasing snow density following Mallett et al., 2020 (version 2.3)

⚠ The monthly snow depth and density fields are available as public data set. (See Section 2.3.2)

## 4.5    Freeboard

Sea-ice freeboard is the height of the sea ice surface above the instantaneous sea surface height. Its estimation requires obtaining the range from the satellite to the snow/ice interface, since it is safe to assume that sea ice in the northern hemisphere is covered with snow in the winter month. The assumption in the AWI CryoSat-2 processing is that the influence of cold and dry snow on Ku-Band radar backscatter and thus the radar range is negligible. There are several studies shedding doubt on this assumption (see 9.1.1), however we maintain this assumption in the absence of a meaningful temporal and regional parametrizations of snow backscatter effects on radar range.

A certain impact by the snow is the slower wave propagation speed of the radar signal in the snow layer. We therefore make the distinction between the terms radar freeboard and freeboard, depending on whether any snow related correction have been applied.

### 4.5.1    Radar Freeboard

The initial radar-derived freeboard is then obtained by subtracting the sea surface height from the sea ice elevation, At this stage the ice elevation is based on a conversion of the two-way travel time into range $r$ with the vacuum light speed and the altitude $alt$ of the satellite

$$elev_{sea\ ice} = r - alt$$
$$rfrb = elev_{sea\ ice} - ssh$$

### 4.5.2    Freeboard

The final step on the freeboard retrieval is the application of a geometric correction that accounts for the slower wave propagation speed of the radar signal in the snow layer. The correction is linear dependent on snow depth and thus implements as a fraction of snow depth and its values is based on the ration of EM wave propagation speed in snow with average density and in vacuum.

$$frb = rfrb + \Delta r_{WP}$$

with

$$\Delta r_{WP} = \left(\frac{c}{c_s} - 1\right) \cdot sd$$
$$c_s = c\,(1 + 0.51\ \times \rho_s)^{-1.5}$$

## 4.6    Sea Ice Density

The knowledge of sea ice density only extends to mean values for first-year (FYI) and multi-year sea ice (MYI) from a limited number of observations (Alexandrov et al., 2010). Sea ice density $\rho_i$ is therefore a parameterization based on the sea ice type auxiliary data, while a fixed value is used for the seawater density (see Table 11).

Table 11: Densities for the sea ice freeboard to thickness conversion

| | | Density (kg/m³) | Uncertainty (kg/m³) | |
|---|---|---|---|---|
| Sea Water | $\rho_W$ | 1024.0 | negligible | |
| First-year sea ice | $\rho_{fyi}$ | 916.7 | $\sigma_\rho^{fyi}$ | 35.7 |
| Multi-year sea ice | $\rho_{myi}$ | 882.0 | $\sigma_\rho^{myi}$ | 23.0 |

$$\rho_i = \rho_{fyi} - f_{myi} \cdot (\rho_{fyi} - \rho_{myi})$$

The uncertainty of sea ice density is therefore a function of the density uncertainties of the pure ice types and the scaling process:

$$\sigma_\rho^i = \sigma_\rho^{fyi} + f_{myi}(\sigma_\rho^{fyi} - \sigma_\rho^{myi}) + \sigma_f^{myi}(\sigma_\rho^{fyi} - \sigma_\rho^{myi})$$

## 4.7 Sea-Ice Thickness

The estimation of sea ice thickness from freeboard is then obtained from the assumption of hydrostatic equilibrium, where the mass of ice and snow equals the mass of displaced seawater.

$$sit = \frac{sd \cdot \rho_S + frb \cdot \rho_W}{\rho_W - \rho_I}$$

The thickness uncertainty depends on all input parameters and is computed by error propagation. The density water varies not significantly and is neglected in the uncertainty budget.

$$\sigma_{sit} = \sqrt{\left(\frac{\rho_w}{\rho_w - \rho_i}\sigma_{frb}\right)^2 + \left(\frac{frb \cdot \rho_w + sd \cdot \rho_s}{(\rho_w - \rho_i)^2}\sigma_\rho^i\right)^2 + \left(\frac{\rho_s}{\rho_w - \rho_i}\sigma_{sd}\right)^2 + \left(\frac{sd}{\rho_w - \rho_i}\sigma_\rho^s\right)^2}$$

## 4.8 Sea Ice Draft

Sea ice draft is defined as $draft = sit - frb$ and its uncertainty is $\sigma_{draft} = \sqrt{\sigma_{sit}^2 + \sigma_{frb}^2}$

## 4.9 Filtering

Several filters are applied to the Level-2 data to remove erroneous data and data section with little data quality confidence:

Table 12: List of data filter for Level-2 processing of trajectory based radar altimeter data

| Filter | Criterion | Action |
|---|---|---|
| Lead tie points | No leads in marine area enclosed by land | *ssh, rfrb, frb, sit* set to NaN in marine area enclosed by land |
| Lead tie points | Distance to next lead tie point > 200 km | *ssh, rfrb, frb, sit* set to NaN for data points |

| Sea-ice Freeboard | *frb* < -0.25m or > 2.25 m | *frb, sit* set to NaN for data points |
|---|---|---|
| Sea-ice thickness | *sit* < -0.5 m or > 10.5 m | *sit* set to NaN for data points |

## 5    Daily Orbit Summaries (Level-2 Pre-Processor)

A daily summary of Level-2 data is generated to provide easy access to CryoSat-2 sea ice altimetry products at the highest possible lateral and temporal resolution. Potential application of this data processing level are the creation of time series for local or customized areas and/or ingestion of freeboard/thickness data without prior temporal or spatial resampling.
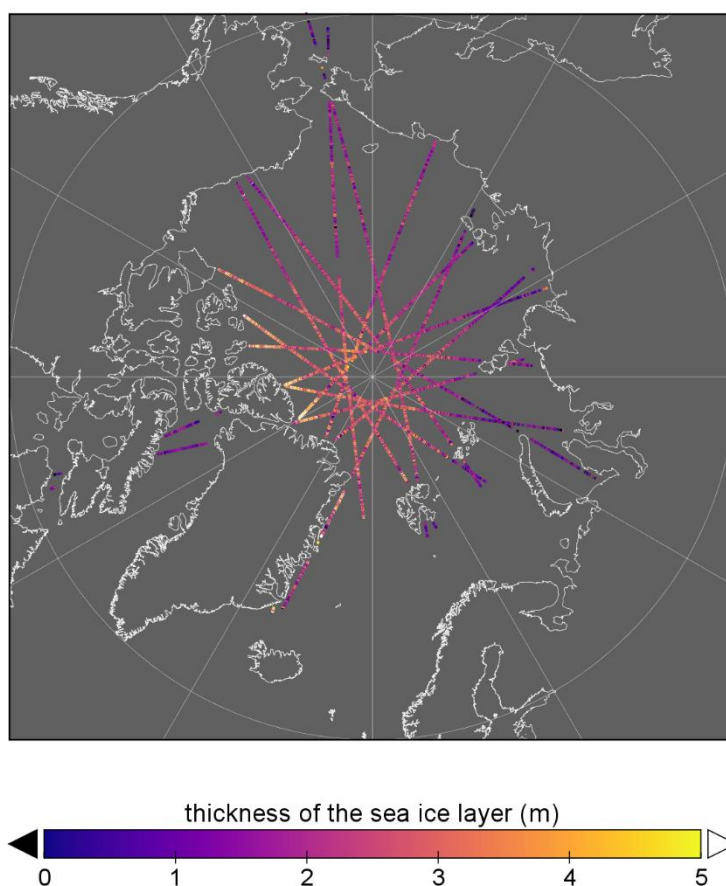


Figure 9: Exemplary data coverage of L2P sea ice thickness points within one day (April 15, 2011)

### 5.1    Data Coverage

The daily L2p file consist of all L2i data points between 00:00:00 – 23:59:59.999 UTC with a valid freeboard value. The geophysical variables are provided as vectors with associated geographical location and their timestamp. A description of the full content can be found in section 7.2.1.

# 6 Colocation on space-time grid (Level-3 Processor)

This section describes how the orbit-based Level-2 data is mapped onto spatiotemporal grids with the Level-3 processor.

## 6.1 Temporal Coverage

Data is gridded for weekly and monthly periods between October 1st and April 30th of each winter season. Specifically, these periods are defined as follows:

Table 13: Definition of periods for gridded products

|  | **Weekly** | **Monthly** |
|---|---|---|
| Start of time coverage | Monday 00:00:00 UTC | First day of month 00:00:00 UTC |
| End of time coverage | Sunday 23:59:59.999 UTC | Last day of month 23:59:59.999 UTC |

The two periods have a different filenaming (see 8.1), the processing is otherwise identical apart the selection of Level-2 input data.  Both outputs therefore share the same processing level (Level 3 collated: L3C).

## 6.2 Grid Definition

The projection is defined as the Equal-Area Scalable Earth Grid version 2 (EASE2-Grid) for the northern hemisphere with a resolution of 25km. The grid resolution has been chosen to provide gapless monthly gridded products in the central Arctic Ocean.

Table 14: Projection used for Level-3 sea ice products in the northern hemisphere

| Property | Value |
|---|---|
| false_easting | 0.0 |
| false_northing | 0.0 |
| grid_mapping_name | lambert_azimuthal_equal_area |
| inverse_flattening | 298.257223563 |
| latitude_of_projection_origin | 90.0 |
| longitude_of_projection_origin | 0.0 |
| proj4_string | +proj=laea +lon_0=0 +datum=WGS84 +ellps=WGS84 +lat_0=90.0 |
| semi_major_axis | 6378137.0 |

Table 15: Grid extent and spacing for Level-3 sea ice products in the northern hemisphere

| Property | Value |
|---|---|
| Grid Dimension | (432, 432) |
| Grid Spacing (km) | 25.0 |
| Grid Notation | Center Coordinates |
| Grid x extent in projection coordinates (km) | (-5387.5, 5387.5) |
| Grid y extent in projection coordinates (km) | (-5387.5, 5387.5) |

⚠ Future product updates may be extent sea-ice thickness retrieval into the southern hemisphere as well

## 6.3   Parameter Gridding

The input processing level for the gridding process are Level-2 intermediate (l2i) files. The positions of all Level-2 data points in these files for the selected period are transformed to projection coordinates and subsequently associated to the index of the corresponding grid cell on the target grid. All geophysical variables of the Level-2 data are than added to parameter stacks for each grid cell.

In general, we apply no filter at this stage, as we assume that Level-2 only contains realistic results.

> ⚠ One exception of the no-filter approach is radar freeboard. The Level-2 notation of radar freeboard also includes measurements over leads, while the freeboard values for these points are NaN. We set radar freeboard values for leads to NaN in the Level-3 processor as otherwise the values of radar freeboard, freeboard and snow depth would not be consistent for gridded data.

Finally, we compute the gridded parameter geophysical $p_{L3}$ based on the stack of Level-2 data ($p_{i,L2}$) using the 'nanmean' function of the python numpy module.

$$p_{L3} = \frac{1}{n_{L2}} \cdot \sum_{i=0}^{n_{L2}} p_{i,L2} \quad if \ p_{i,L2} \neq NaN$$

The following Level-2 parameters are gridded using the average method:

1. radar freeboard
2. freeboard
3. sea ice thickness
4. sea level anomaly
5. mean sea surface
6. snow depth
7. snow density
8. sea ice density
9. sea ice type
10. sea ice concentration

## 6.4   Uncertainty of Gridded Parameters

The process of averaging reduces random errors in observations, however not all error contributions in the sea-ice thickness retrieval are random (Ricker et al., 2014). Since all geophysical variables in the Level-2 data have an associated uncertainty, the Level-3 processor provides a corresponding uncertainty variable for gridded data and different strategies are in place depending on the nature of the error.

### 6.4.1   Systematic Uncertainties

The Level-3 uncertainty representation for systematic errors (e.g. snow depth, sea ice density) is the average of the Level-2 uncertainty and computed in the same way as the geophysical variables in the section 6.3.

### 6.4.2   Random Uncertainties

The gridded uncertainty of parameters with only random uncertainty is computed as the error of the weighted mean, since we have individual uncertainties for each value contributing to the gridded mean.

$$\hat{\sigma} = \sqrt{\sum_{n_{L2}} \frac{1}{(\sigma_{L2})^2}}^{-1}$$

This approach applies only to the radar freeboard, whose two error contributions range noise and sea surface height interpolation uncertainty are both defined as random error contributions.

⚠ To maintain consistency with older versions of the data set, the average of the Level-2 radar freeboard uncertainty is also provided under the variable name `radar_freeboard_l2_uncertainty`

### 6.4.3    Mixed Systematic and Random Uncertainties

Level-2 parameter uncertainties that based on error propagation with both random and systematic error contributions, such as those of freeboard or sea ice thickness, however, cannot easily be transferred to gridded uncertainties via gridding as this overestimates the error. The error of the weighted mean is also not an option as it essentially reduces the uncertainty to zero for grid cells with significant amounts of Level-2 data points.

We therefore re-compute the error propagation of freeboard and thickness with the stacks of all geophysical variables the uncertainties and use average ($\bar{\sigma}$) or weighed mean error ($\hat{\sigma}$) where appropriate.

This results in Level-3 uncertainty computations for freeboard:

$$\sigma_{l3,frb} = \sqrt{\left(\Delta r_{WP} \cdot \bar{\sigma}_{sd}\right)^2 + \left(\hat{\sigma}_{rfrb}\right)^2}$$

and thickness:

$$\sigma_{l3,sit} = \sqrt{\left(\frac{\bar{\rho}_w}{\bar{\rho}_w - \bar{\rho}_i}\sigma_{l3,frb}\right)^2 + \left(\frac{\overline{frb} \cdot \bar{\rho}_w + \overline{sd} \cdot \bar{\rho}_s}{(\bar{\rho}_w - \bar{\rho}_i)^2}\bar{\sigma}_\rho^i\right)^2 + \left(\frac{\bar{\rho}_s}{\bar{\rho}_w - \bar{\rho}_i}\bar{\sigma}_{sd}\right)^2 + \left(\frac{\overline{sd}}{\bar{\rho}_w - \bar{\rho}_i}\bar{\sigma}_\rho^s\right)^2}$$

⚠ To maintain consistency with older versions of the data set, the average of the Level-2 freeboard and thickness uncertainties are also provided under the variable names `freeboard_l2_uncertainty` and `sea_ice_thickness_l2_uncertainty`

## 6.5    Grid-Cell Statistics

### 6.5.1    Spatial Coverage per grid cell

The orbit coverage and the varying skill of the surface type classification algorithm in the Level-2 processor yields a wide range of number of samples for the gridding. The orbit coverage is increasing non-linear with latitude with a maximum at 88N. Here the point density is several magnitudes greater than at the southern sea ice limit. The number of classified waveforms is generally lower over sea ice surface with a large degree of surface-type mixing with the CryoSat-2 footprint.

These effects are documented by a set of grid-cell statistical parameters shown in Figure 10 and defined in Table 16.
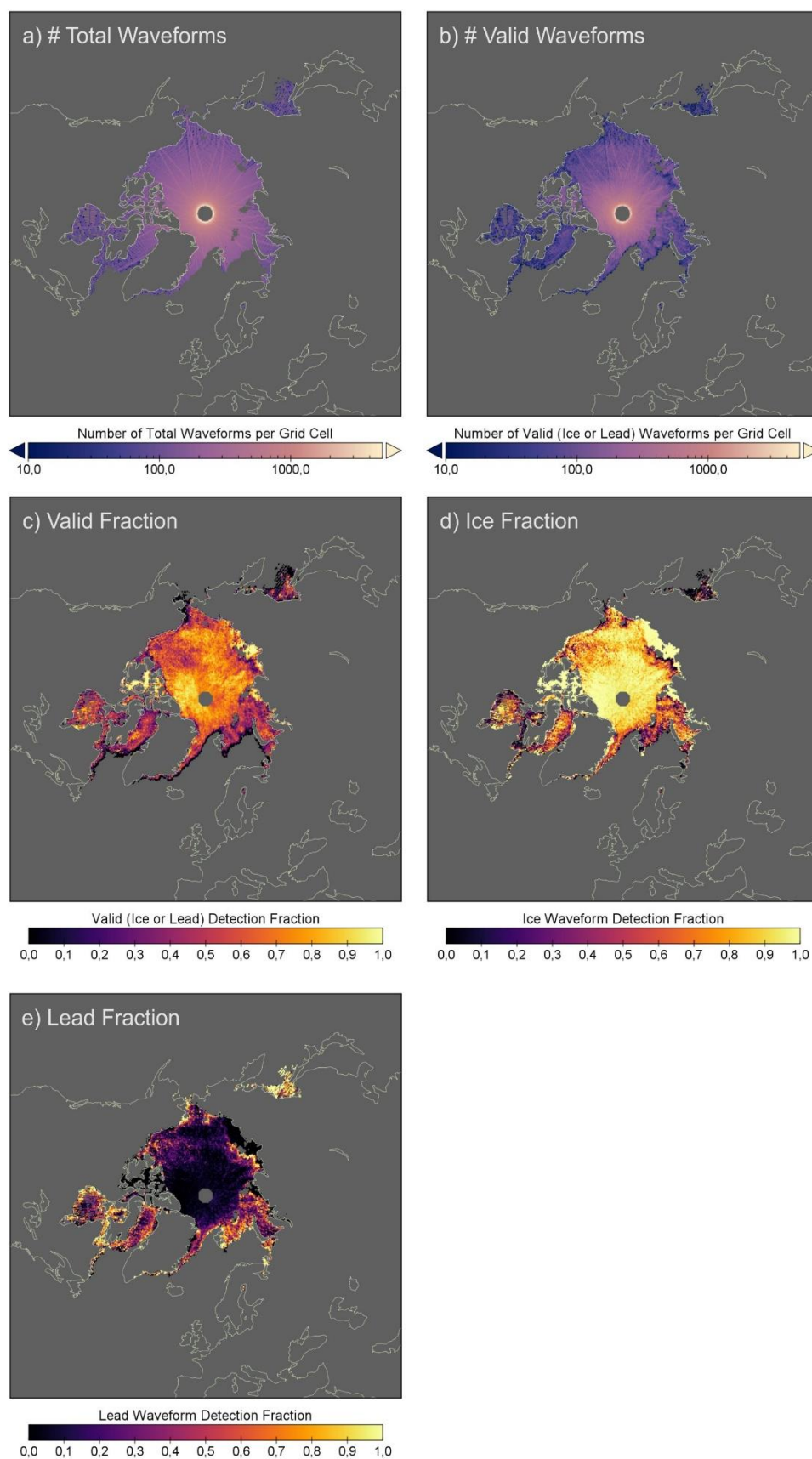
Figure 10: Example of Level-3 grid cell statistics: a) number of all waveforms per grid cell, b) number of valid waveforms classified as either ice or lead, c) fraction of ice or lead waveforms to total waveforms, d) fraction of ice detections in valid waveforms and e) number of lead detections in valid waveforms

Table 16: Definition of Level-3 grid cell statistics

| Parameter | Definition | Comment |
|---|---|---|
| Number of total waveforms | $N_{twf}$ | All Level-1 waveforms |
| Number of valid waveforms | $N_{vwf}$ | All Level-1 waveforms that are positively classified as either ice or lead surfaces |
| Valid Fraction | $f_{vf} = N_{vwf}/N_{twf}$ | |
| Ice Fraction | $f_{ice} = N_{ice}/N_{vwf}$ | $N_{ice}$: Number of waveforms classified as ice |
| Lead Fraction | $f_{lead} = N_{lead}/N_{vwf}$ | $N_{lead}$: Number of waveforms classified as leads |

### 6.5.2   Temporal Coverage per grid cell

Additional grid statistics parameter have been added in version 2.2 of the AWI sea ice product. The number of orbits contributing to each grid cell in a weekly or monthly period is not uniform and depends on its location. It is therefore not guaranteed that each grid cell contains a full temporal coverage especially for monthly periods. The result of a non-uniform temporal distribution may be a sea ice thickness phase base if the actual coverage is centered only on the beginning or end of the grid period.

The Level-3 processor keeps track of the date of each along-track sea-ice thickness observation and computes four statistical parameters (see Figure 11), which are computed for each grid cell.

⚠ The temporal statistics are limited only to sea-ice thickness

#### 6.5.2.1   Uniformity Factor

The uniformity factor describes how close the collection of observations follows a uniform distribution, e.g. if all days in the grid period contribute equally the grid cells mean sea-ice thickness values. A value of 1 indicates a uniform distribution, while a value close to 0 occurs if only the first or last day in the grid period has sea-ice thickness data.

The factor is computed with by Kolmogorov-Smirnov (KS) test that evaluates the distribution of contributing days against a uniform distribution. As the result of the KS test (D value) converges towards 0 for matching distributions, the uniformity factor is defined as *1 – D.*

#### 6.5.2.2   Daily Coverage Fraction

The daily fraction coverage indicates how many days in the full grid period contribute to the average sea-ice thickness result (defined as: *number of days with SIT / number of days in full grid period*).

### 6.5.3   First to Last Day Coverage Fraction

This statistic is similar to the daily coverage fraction, but indicates the fraction of the grid period between the first and last day with sea-ice thickness observations (defined as: *(last day with SIT – first day with SIT) / number of days in full grid period*).

### 6.5.3.1 Center of Coverage

This parameter indicates the center of sea-ice thickness in the temporal domain by computing the average date of all sea-ice thickness observations relative to the grid period. E.g. the center of a uniform distribution is the center of the period (0.5), while values of 0 and 1 indicates observations only from the beginning or end of the grid period, respectively. This parameter can be used to estimate potential sea-ice thickness phase biases on grid cell basis.
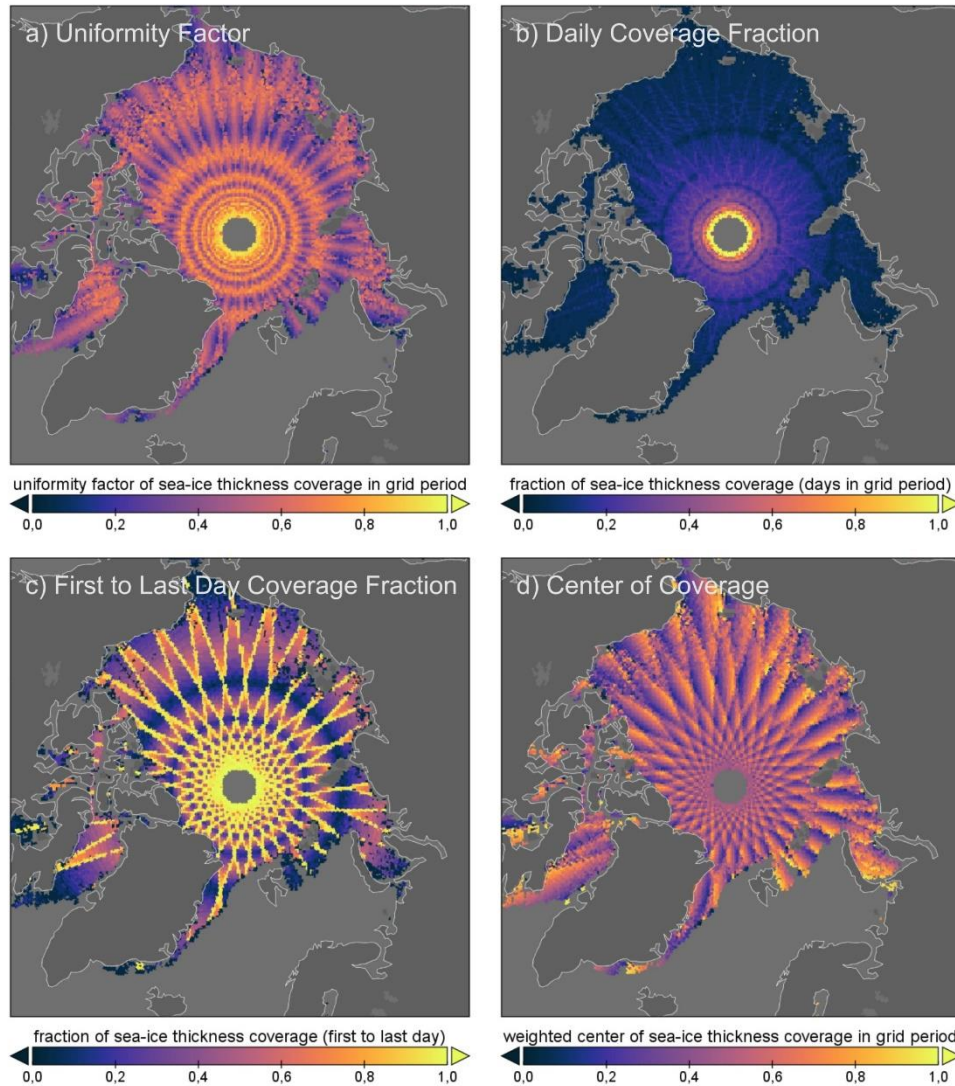


Figure 11: Temporal coverage statistics of sea-ice thickness per grid cell.

## 6.6 Flags and Masks

Level-3 products contain flags and masks to inform the user on the outcome of the retrieval and other boundary conditions for each grid cell. Figure 12 and in the subsections below give an overview of all flags in the Level-3 data products.

### 6.6.1    Status Flag

The status flag provides information on the availability of Level-2 input data, the sea/land mask and the success/failure of the retrieval. The flag value (Table 17) is unique for each grid cell.

Table 17: Status flag values and meaning of Level-3 status flag

| Flag Value | Flag Meaning |
|---|---|
| 0 | Nominal sea ice thickness retrieval |
| 1 | no input data |
| 2 | outside sea ice concentration mask (open ocean) |
| 3 | latitude above orbit inclination |
| 4 | land, lake or land ice |
| 5 | sea ice thickness retrieval failed |

⚠ Future product updates may be changing the value of the status flag to be compliant with the convention that the flag value 0 indicated nominal retrieval

### 6.6.2    Quality Flag

The quality flag represents an educated guess of the performance of the sea-ice thickness retrieval based on several parameters and statistics. Other than the sea-ice thickness uncertainty, the quality flag is dependent also on data from adjacent grid cells. The conditions detailed in Table 18 are the basis for computing flag values in Table 19. The resulting quality flag for a given grid cell is always the lowest value/quality from the set of conditions.

Table 18: Conditions for quality flag values

| Quality Flag | Criterion |
|---|---|
| Low | Less than 10 Level-2 thickness data points per grid cell |
| Low | Negative thickness fraction > 40% |
| Intermediate | CryoSat-2 in SARin mode |
| Intermediate | Area lead fraction (the maximum lead fraction in grid cells with 75 km search radius) < 10% |
| Intermediate | Less than 10 Level-2 thickness data points per grid cell |
| Intermediate | Negative thickness fraction between 20% - 40% |
| Nominal | None of the above |

Table 19: Quality flag values and meaning for Level-3 products

| Flag Value | Flag Meaning |
|---|---|
| 0 | nominal quality |
| 1 | intermediate quality |
| 2 | low Quality |
| 3 | no input data |

### 6.6.3    Radar Mode

CryoSat-2 data consists of two radar modes and their regional distribution can be traced with the radar mode mask in Level-3 products. For a given grid-cell the mask value is based on the median of the number of SAR/SARin Level-2 data points as the mode mask changes can happen within a grid cell. The mask therefore indicates which radar mode has the majority of points per grid cell and not their fractions.

Table 20 Radar mode flag values and meaning

| Flag Value | Flag Meaning |
|---|---|
| 0 | Pulse-limited/LRM (not used) |
| 1 | SAR |
| 2 | SAR interferometric (SARin) |

### 6.6.4    Region

Each grid-cell with sea ice coverage is associated to a certain region. The definition of the region is a variant of the NSIDC regions of the Arctic Ocean[4]. Here, the region definition for the central Arctic Ocean is identical to the NSIDC one, only the region of the Baltic Sea has been added for the AWI CryoSat-2 product.

Table 21: Region ID flag value and meaning

| Flag Value | Flag Meaning | Flag Value | Flag Meaning |
|---|---|---|---|
| 0 | Inland sea and lakes (not used) | 12 | Chukchi Sea |
| 1 | Ice-free Oceans | 13 | Beaufort Sea |
| 2 | Sea of Okhotsk | 14 | Canadian Islands |
| 3 | Bering | 15 | Central Arctic |
| 4 | Hudson Bay | 16 | Baltic Sea |
| 5 | St John | 17 | not used |
| 6 | Baffin Bay | 18 | not used |
| 7 | East Greenland Sea | 19 | not used |
| 8 | Barents Sea | 20 | land |
| 9 | Kara Sea | 21 | Land outline (not used) |
| 10 | Laptev Sea | | |
| 11 | East Siberian Sea | | |

---

[4] http://nsidc.org/arcticseaicenews/map-of-the-arctic-ocean/
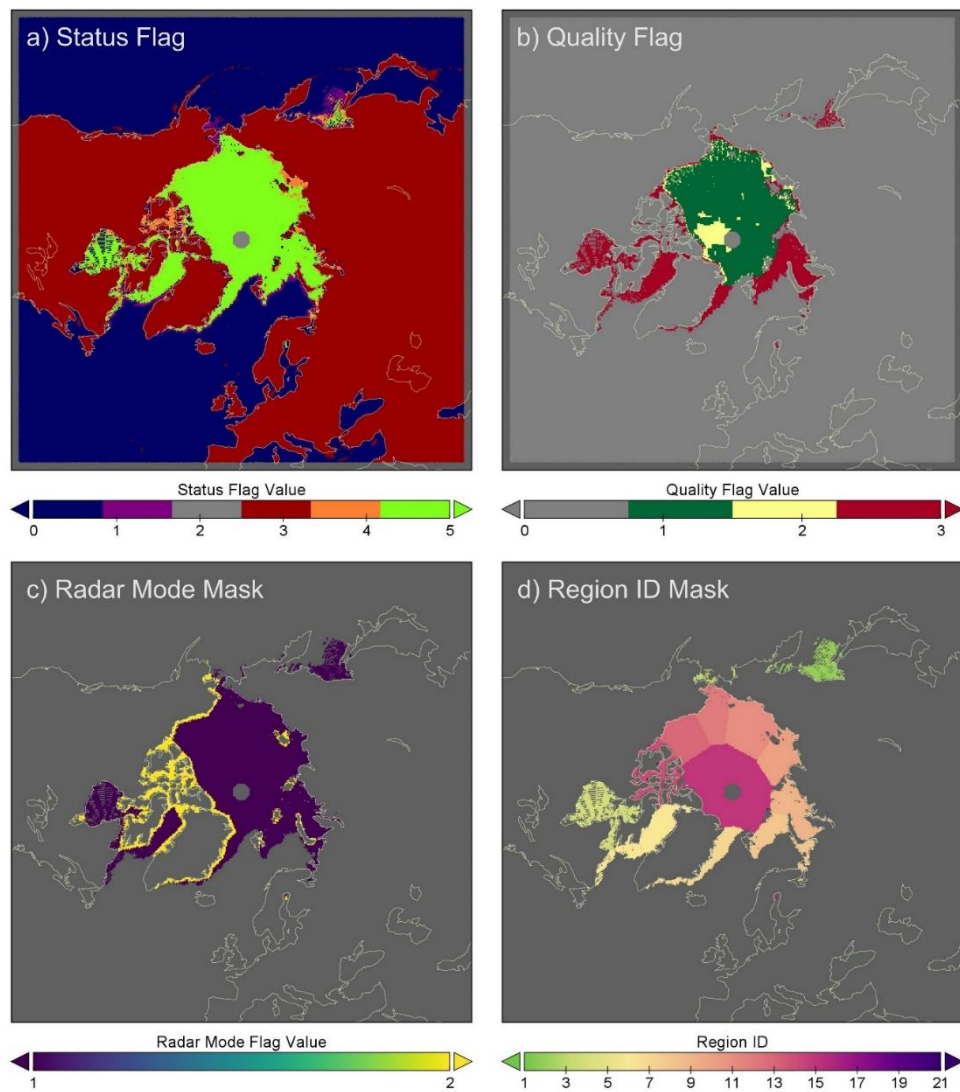
Figure 12: Examples of flags and masks in gridded Level-3 product (April 2018). a) Retrieval status flag, b) Retrieval quality flag, c) mask indicating SAR/SARin source data and d) Regions of the Arctic Ocean and Sub-arctic Seas (variant of NSIDC region mask).

# 7 Product Specification

This section provided the technical specifications of the output products.

## 7.1 File Format

### 7.1.1 netCDF

All product files are provided in Network Common Data Format (NetCDF) in version 4. NetCDF is a scientific data format that is platform independent and can be parsed with any major programming language. The format also combines data and metadata, and for the latter we use the conventions for CF (Climate and Forecast) metadata.

> 💡 Please see section 8.2 for visualization of NetCDF files

### 7.1.2 GeoTIFF

Sea-ice thickness from gridded products is also available as geotiff files with the same projection and extent as the netCDF files. Filenaming is identical to the netCDF files except the file suffix (.tiff) and the geotiff output can be found in the same folder structure.

## 7.2 Processing Levels

### 7.2.1 Trajectory Level-2 Pre-processed (l2p)

#### 7.2.1.1 Filenaming

The filenames of trajectory-based products contain the following information:

```
awi-siral-l2p-sithick-cryosat2-<timeliness>-<hemisphere>-<period>-fv2p4.nc
```
where:

| | |
|---|---|
| `<timeliness>` | "nrt" or "rep" |
| `<hemisphere>` | "nh" |
| `<period>` | "YYYYMMDD " |

#### 7.2.1.2 Global Attributes

Table 22: List of global attributes and their values of L2P NetCDF files

| Attribute | Value |
|---|---|
| `title` | "Collection of daily geophysical & auxiliary sea ice parameters from satellite radar altimetry at footprint resolution" |
| `institution` | "Alfred-Wegener-Institut Helmholtz Zentrum für Polar und Meeresforschung (AWI)" |

| Attribute | Value |
|---|---|
| source | "Altimetry: CryoSat-2 Level 1b baseline D/E (ipf1-d/e), Snow depth: Monthly climatology based on regional merging of Warren Climatology with 50% reduction for first-year sea ice in the central Arctic and AMSR-2 based snow depth from IUP Bremen in remaining ice-covered regions, Mean Sea Surface: DTU21 global mean sea surface, Sea ice Concentration: OSI-SAF (OSI-401-b), Sea ice type: OSI-SAF (OSI-403-d), Region code: Adapted from NSIDC region mask" |
| platform | "CryoSat-2" |
| sensor | "SIRAL" |
| history | "<timestamp> - Product generated with pysiral version <software_version>" |
| references | <this-document> |
| tracking_id | "<uuid string>" |
| conventions | "CF-1.6" |
| product_version | "2.4" |
| processing_level | "Level-3 Collated (l3c)" |
| summary | "This dataset contains Level-3 monthly sea ice thickness products from satellite observations in the northern hemisphere. Level-3 data are raw observations processed to geophysical quantities and placed onto a regular grid." |
| topiccategory | "Oceans Climatology Meteorology Atmosphere" |
| keywords | "Earth Science > Cryosphere > Sea Ice > Ice Depth/Thickness, Earth Science > Oceans > Sea Ice > Ice Depth/Thickness, Earth Science > Climate Indicators > Cryospheric Indicators > Ice Depth/Thickness, Geographic Region > Northern Hemisphere, Vertical Location > Sea Surface, Institutions > AWI > Alfred Wegener Institute for Polar and Marine Research" |
| id | "awi-siral-l2p-sithick-cryosat2-<timeliness>-<hemisphere>-<period>-fv2p4" |
| naming_authority | "de.awi" |
| keywords_vocabulary | "GCMD Science Keywords" |
| doi | "None" |
| cdm_data_type | "Trajectory" |
| comment | "Data points only for valid freeboard retrievals" |
| date_created | <timestamp> |
| creator_name | "Alfred-Wegener-Institut Helmholtz Zentrum für Polar und Meeresforschung" |
| creator_type | "institution" |
| creator_url | " https://spaces.awi.de/display/SIRAL/" |
| contributor_name | "Stefan Hendricks, Robert Ricker, Stephan Paul" |
| contributor_role | "PrincipalInvestigator, Author, Author" |
| project | "AWI Sea Ice Radar Altimetry (SIRAL)" |
| publisher_name | "Alfred-Wegener-Institut Helmholtz Zentrum für Polar und Meeresforschung" |
| publisher_url | "www.awi.de" |
| publisher_email | "cs2smos-support@awi.de" |
| time_coverage_start | "<tcs>" of form YYYY-MM-DDTHH:MI:SS.SSSSSS |
| time_coverage_end | "<tce>" of form YYYY-MM-DDTHH:MI:SS.SSSSSS |
| time_coverage_duration | "P1D" |
| time_coverage_resolution | "P1D" |
| standard_name_vocabulary | "CF Standard Name Table (v36, 21 September 2016)" |
| license | "Creative Commons Attribution 4.0 International (CC BY 4.0)" |

### 7.2.1.3 Geophysical Variables

Table 23: List of all variables (in alphabetical order) and their dimensions of L2P NetCDF files

| Variable | Attributes |
|---|---|
| sea_ice_freeboard | double |
| | long_name = "freeboard of the sea ice layer"; |
| | standard_name = "sea_ice_freeboard"; |
| | units = "m"; |
| | coordinates = "time"; |
| sea_ice_freeboard_uncertainty | float |
| | standard_name = "sea_ice_freeboard standard_error"; |
| | long_name = "freeboard uncertainty"; |
| | units = "m"; |
| | coordinates = "time"; |
| radar_freeboard | double |
| | long_name = "elevation of retracked point above instantaneous sea surface height"; |
| | comment = "radar freeboard is defined as the elevation based on the assumption of vacuum light speed without a snow propagation or range penetration correction"; |
| | units = "m"; |
| | coordinates = "time"; |
| radar_freeboard_uncertainty | double |
| | coordinates = "time"; |
| | long_name = "algorithm uncertainty (error propagation) of the radar freeeboard retrieval"; |
| | units = "m"; |
| radar_mode | double |
| | coordinates = "time"; |
| | flag_meanings = "pulse_limited_lrm doppler_delay_sar doppler_delay_sar_interferometric"; |
| | flag_values = "0, 1, 2"; |
| | long_name = "radar mode flag"; |
| | units = "1"; |
| | valid_max = 2.0; // double |
| | valid_min = 0.0; // double |
| region_code | double |
| | comment = "Added flag for Baltic Sea (flag value 16)"; |
| | coordinates = "time"; |
| | flag_meanings = "inland_sea_and_lakes ice_free_oceans sea_of_okhotsk bering hudson_bay st_john baffin_bay east_greenland_sea barents_sea kara_sea laptev_sea east_siberian_sea chukchi_sea beaufort_sea canadian_islands central_arctic valtic_sea land land_outline"; |
| | flag_values = "0, 1, 2, 3, 4, 5, 6, 7, 8, 9, 10, 11, 12, 13, 14, 15, 16, 20, 21"; |
| | long_name = "Region code (adapted from NSIDC region mask)"; |
| | units = "1"; |
| | valid_max = 21.0; // double |
| | valid_min = 0.0; // double |

| Variable | Attributes |
|---|---|
| sea_ice_density | Double |
| | standard_name = "sea_ice_density"; |
| | long_name = "density of the sea ice layer"; |
| | units = "kg m-3"; |
| | coordinates = "time"; |
| sea_ice_density_uncertainty | double |
| | long_name = "uncertainty of the sea ice layer density"; |
| | standard_name = "sea_ice_density standard_error"; |
| | coordinates = "time"; |
| | units = "kg m-3"; |
| sea_ice_thickness | Double |
| | long_name = "thickness of the sea ice layer"; |
| | standard_name = "sea_ice_thickness"; |
| | units = "m"; |
| | coordinates = "time"; |
| sea_ice_thickness_uncertainty | double |
| | long_name = "uncertainty of the sea ice layer thickness"; |
| | units = "m"; |
| | standard_name = "sea_ice_thickness_uncertainty"; |
| | coordinates = "time"; |
| sea_ice_type | double |
| | valid_max = 1.0; // double |
| | valid_min = 0.0; // double |
| | coordinates = "time"; |
| | long_name = "fraction of multi-year ice (0: only first year ice, 1: only multi-year ice)"; |
| | standard_name = "sea_ice_classification"; |
| | units = "1"; |
| sea_ice_type_uncertainty | double sea_ice_type_uncertainty |
| | long_name = "uncertainty of sea ice classification"; |
| | standard_name = "sea_ice_classification standard_error"; |
| | units = "1"; |
| | coordinates = "time"; |
| snow_density | Double |
| | long_name = "density of the snow layer"; |
| | units = "kg m-3"; |
| | coordinates = "time"; |
| snow_density_uncertainty | Double |
| | coordinates = "time"; |
| | long_name = "uncertainty of the snow layer density"; |
| | units = "kg m-3"; |
| snow_depth | Double |
| | coordinates = "time"; |
| | long_name = "thickness of the snow layer"; |
| | standard_name = "snow_depth"; |
| | units = "m"; |

| Variable | Attributes |
|----------|------------|
| `snow_depth_uncertainty` | `Double` |
| | `coordinates = "time";` |
| | `long_name = "uncertainty of the snow layer thickness";` |
| | `standard_name = "snow_depth standard_error";` |
| | `units = "m";` |

### 7.2.1.4   Coordinates

| Metadata Variables | Attributes |
|--------------------|------------|
| `latitude` | `Float` |
| | `units = "degrees north";` |
| | `long_name = "latitude of satellite nadir measurement point";` |
| | `standard_name = "latitude";` |
| | `coordinates = "time";` |
| `longitude` | `Float` |
| | `units = "degrees east";` |
| | `long_name = "longitude of satellite nadir measurement point";` |
| | `standard_name = "longitude";` |
| | `coordinates = "time";` |
| `time` | `double` |
| | `units = "seconds since 1970-01-01";` |
| | `long_name = "utc timestamp";` |

### 7.2.2     Space-time grid Level-3 Colated (l3c)

### 7.2.2.1   Filenaming

The filenames of gridded products contain the following information:

    `awi-siral-l3c-sithick-cryosat2-<timeliness>-<grid_id>-<period>-fv2p4.nc`
where:

| `<timeliness>` | "nrt" or "rep" |
|----------------|----------------|
| `<grid_id>` | "nh_25km_ease2" |
| `<period>` | "YYYYMMDD_YYYYMMDD"  (weekly product: start & end date)<br>"YYYYMM"                   (monthly product) |

> ☼ Start and end date for weekly products will always be Monday through Sunday. Times in UTC

### 7.2.2.2   Global Attributes

Table 24: List of global attributes and their values of L3C NetCDF files

| Attribute | Value |
|-----------|-------|
| `title` | `"Monthly gridded sea-ice thickness and auxiliary parameters from satellite radar altimeter data"` |
| `institution` | `"Alfred-Wegener-Institut Helmholtz Zentrum für Polar und Meeresforschung (AWI)"` |

| Attribute | Value |
|---|---|
| source | "Altimetry: CryoSat-2 Level 1b baseline E (ipf1-e), Snow depth: Monthly climatology based on regional merging of Warren Climatology with 50% reduction for first-year sea ice in the central Arctic and AMSR-2 based snow depth from IUP Bremen in remaining ice-covered regions, Mean Sea Surface: DTU21 global mean sea surface, Mean Dynamic Topography: DTU17, Sea ice Concentration: C3S, Sea Ice Concentration CDR/ICDR, Sea ice type: C3S Sea Ice Type CDR/ICDR, Region code: Adapted from NSIDC region mask" " |
| platform | "CryoSat-2" |
| sensor | "SIRAL" |
| history | "<timestamp> - Product generated with pysiral version <software_version>" |
| references | <this document> |
| tracking_id | "<uuid string>" |
| conventions | "CF-1.6" |
| product_version | "2.4" |
| processing_level | "Level-3 Collated (l3c)" |
| summary | "This dataset contains Level-3 monthly sea ice thickness products from satellite observations in the northern hemisphere. Level-3 data are raw observations processed to geophysical quantities and placed onto a regular grid." |
| topiccategory | "Oceans Climatology Meteorology Atmosphere" |
| keywords | "Earth Science > Cryosphere > Sea Ice > Ice Depth/Thickness, Earth Science > Oceans > Sea Ice > Ice Depth/Thickness, Earth Science > Climate Indicators > Cryospheric Indicators > Ice Depth/Thickness, Geographic Region > Northern Hemisphere, Vertical Location > Sea Surface, Institutions > AWI > Alfred Wegener Institute for Polar and Marine Research" |
| id | "awi-siral-l3-cryosat2-nrt-nh_25km_ease2-<tcs>-<tce>-fv2p4" |
| naming_authority | "de.awi" |
| keywords_vocabulary | "GCMD Science Keywords" |
| doi | "None" |
| cdm_data_type | "Grid" |
| comment | "Northern hemisphere sea ice thickness coverage is limited to the winter month between October and April due to negative effect of surface melt on the retrieval of freeboard." |
| date_created | <timestamp> |
| creator_name | "Alfred-Wegener-Institut Helmholtz Zentrum für Polar und Meeresforschung" |
| creator_type | "institution" |
| creator_url | " https://spaces.awi.de/display/SIRAL/" |
| contributor_name | "Stefan Hendricks, Robert Ricker, Stephan Paul" |
| contributor_role | "PrincipalInvestigator, Author, Author" |
| project | "AWI Sea Ice Radar Altimetry (SIRAL)" |
| publisher_name | "Alfred-Wegener-Institut Helmholtz Zentrum für Polar und Meeresforschung" |
| publisher_url | "www.awi.de" |
| publisher_email | "cs2smos-support@awi.de" |
| geospatial_lat_min | "16.6239" |
| geospatial_lat_max | "90.0" |
| geospatial_lon_min | "-180.0" |
| geospatial_lon_max | "180.0" |

| Attribute | Value |
|---|---|
| geospatial_vertical_min | "0.0" |
| geospatial_vertical_max | "0.0" |
| spatial_resolution | "25km grid spacing" |
| geospatial_bounds_crs | "EPSG:6931" |
| time_coverage_start | "<tcs>" of form YYYY-MM-DDTHH:MI:SS.SSSSSS |
| time_coverage_end | "<tce>" of form YYYY-MM-DDTHH:MI:SS.SSSSSS |
| time_coverage_duration | "P1M" for monthly, "P7D" for weekly |
| time_coverage_resolution | "P1M" for monthly, "P7D" for weekly |
| standard_name_vocabulary | "CF Standard Name Table (v36, 21 September 2016)" |
| license | "Creative Commons Attribution 4.0 International (CC BY 4.0)" |

### 7.2.2.3   Geophysical Variables

Table 25: List of all variables (in alphabetical order) and their dimensions of L3C NetCDF files

| Variable | Attributes |
|---|---|
| sea_ice_freeboard | double (time=1, yc=432, xc=432); |
|  | :coverage_content_type = "physicalMeasurement"; |
|  | long_name = "freeboard of the sea ice layer"; |
|  | standard_name = "sea_ice_freeboard"; |
|  | units = "m"; |
|  | grid_mapping = "Lambert_Azimuthal_Grid"; |
|  | coordinates = "time lat lon"; |
| sea_ice_freeboard_uncertainty | float (time=1, yc=432, xc=432); |
|  | :coverage_content_type = "physicalMeasurement"; |
|  | standard_name = "sea_ice_freeboard standard_error"; |
|  | long_name = "algorithm uncertainty (error propagation) of the sea ice freeboard retrieval (computed as error of a weighted mean)"; |
|  | units = "m"; |
|  | grid_mapping = "Lambert_Azimuthal_Grid"; |
|  | coordinates = "time lat lon"; |
| sea_ice_thickness | double (time=1, yc=432, xc=432); |
|  | :coverage_content_type = "physicalMeasurement"; |
|  | long_name = "thickness of the sea ice layer"; |
|  | standard_name = "sea_ice_thickness"; |
|  | units = "m"; |
|  | grid_mapping = "Lambert_Azimuthal_Grid"; |
|  | coordinates = "time lat lon"; |
| sea_ice_thickness_uncertainty | double (time=1, yc=432, xc=432); |
|  | :coverage_content_type = "physicalMeasurement"; |
|  | long_name = "uncertainty of the sea ice layer thickness"; |
|  | units = "m"; |
|  | standard_name = "sea_ice_thickness_uncertainty"; |
|  | grid_mapping = "Lambert_Azimuthal_Grid"; |
|  | coordinates = "time lat lon"; |
| sea_ice_draft | double (time=1, yc=432, xc=432); |
|  | :coverage_content_type = "physicalMeasurement"; |

| | |
|---|---|
| | coordinates = "time lat lon"; |
| | long_name = "depth of the sea-ice layer below the water surface"; |
| | standard_name = "sea_ice_classification"; |
| | grid_mapping = "Lambert_Azimuthal_Grid"; |
| | units = "m"; |
| sea_ice_draft_uncertainty | double (time=1, yc=432, xc=432); |
| | :coverage_content_type = "physicalMeasurement"; |
| | coordinates = "time lat lon"; |
| | long_name = "algorithm uncertainty (error propagation) of sea ice draft including uncertainty reduction of random components by gridding"; |
| | standard_name = "sea_ice_draft"; |
| | grid_mapping = "Lambert_Azimuthal_Grid"; |
| | units = "1"; |
| sea_ice_type | double (time=1, yc=432, xc=432); |
| | :coverage_content_type = "auxiliaryInformation"; |
| | valid_max = 1.0; // double |
| | valid_min = 0.0; // double |
| | coordinates = "time lat lon"; |
| | long_name = "fraction of multi-year ice (0: only first year ice, 1: only multi-year ice)"; |
| | standard_name = " sea_ice_draft standard_error"; |
| | grid_mapping = "Lambert_Azimuthal_Grid"; |
| | units = "1"; |
| sea_ice_type_uncertainty | double (time=1, yc=432, xc=432); |
| | :coverage_content_type = "auxiliaryInformation"; |
| | long_name = "uncertainty of sea ice classification"; |
| | standard_name = "sea_ice_classification standard_error"; |
| | units = "1"; |
| | grid_mapping = "Lambert_Azimuthal_Grid"; |
| | coordinates = "time lat lon"; |
| sea_level_anomaly | float(time=1, yc=432, xc=432); |
| | :coverage_content_type = "physicalMeasurement"; |
| | long_name = "departure of instantaneous sea surface height from mean sea surface height"; |
| | units = "m"; |
| | grid_mapping = "Lambert_Azimuthal_Grid"; |
| | standard_name = "sea_surface_height_above_mean_sea_level"; |
| | coordinates = "time lat lon"; |
| sea_level_anomaly_uncertainty | float (time=1, yc=432, xc=432); |
| | :coverage_content_type = "physicalMeasurement"; |
| | long_name = "uncertainty of instantaneous sea surface height"; |
| | standard_name = "sea_surface_height_above_mean_sea_level standard_error"; |
| | coordinates = "time lat lon"; |
| | grid_mapping = "Lambert_Azimuthal_Grid"; |
| | units = "m"; |
| mean_sea_surface | float mean_sea_surface(time=1, yc=432, xc=432); |
| | :coverage_content_type = "auxiliaryInformation"; |
| | standard_name = "sea_surface_height_above_reference_ellipsoid"; |

| | |
|---|---|
| | coordinates = "time lat lon"; |
| | grid_mapping = "Lambert_Azimuthal_Grid"; |
| | long_name = "elevation of mean sea surface at measurement point (above WGS84 ellipsoid)"; |
| | units = "m"; |
| radar_freeboard | double (time=1, yc=432, xc=432); |
| | :coverage_content_type = "physicalMeasurement"; |
| | grid_mapping = "Lambert_Azimuthal_Grid"; |
| | long_name = "elevation of retracked point above instantaneous sea surface height (no snow range corrections)"; |
| | coordinates = "time lat lon"; |
| | units = "m"; |
| | grid_mapping = "Lambert_Azimuthal_Grid"; |
| radar_freeboard_uncertainty | double (time=1, yc=432, xc=432); |
| | :coverage_content_type = "physicalMeasurement"; |
| | coordinates = "time"; |
| | long_name = "algorithm uncertainty (error propagation) of the radar freeeboard retrieval"; |
| | grid_mapping = "Lambert_Azimuthal_Grid"; |
| | coordinates = "time lat lon"; |
| snow_density | double (time=1, yc=432, xc=432); |
| | :coverage_content_type = "auxiliaryInformation"; |
| | long_name = "density of the snow layer"; |
| | units = "kg m-3"; |
| | grid_mapping = "Lambert_Azimuthal_Grid"; |
| | coordinates = "time lat lon"; |
| snow_density_uncertainty | Double (time=1, yc=432, xc=432); |
| | :coverage_content_type = "auxiliaryInformation"; |
| | coordinates = "time lat lon"; |
| | long_name = "uncertainty of the snow layer density"; |
| | grid_mapping = "Lambert_Azimuthal_Grid"; |
| | units = "kg m-3"; |
| snow_depth | Double (time=1, yc=432, xc=432); |
| | :coverage_content_type = "auxiliaryInformation"; |
| | coordinates = "time lat lon"; |
| | long_name = "thickness of the snow layer"; |
| | standard_name = "snow_depth"; |
| | grid_mapping = "Lambert_Azimuthal_Grid"; |
| | units = "m"; |
| snow_depth_uncertainty | Double (time=1, yc=432, xc=432); |
| | :coverage_content_type = "auxiliaryInformation"; |
| | coordinates = "time lat lon"; |
| | long_name = "uncertainty of the snow layer thickness"; |
| | standard_name = "snow_depth standard_error"; |
| | grid_mapping = "Lambert_Azimuthal_Grid"; |
| | units = "m"; |

### 7.2.2.4 Grid Statistics

| Variable | Attributes |
|---|---|
| stat_ice_fraction | float (time=1, yc=432, xc=432); |
| | :coverage_content_type = "qualityInformation"; |
| | grid_mapping = "Lambert_Azimuthal_Grid"; |
| | long_name = "sea ice waveform detections per valid waveforms in grid cell"; |
| | coordinates = "time lat lon"; |
| | units = "1"; |
| | grid_mapping = "Lambert_Azimuthal_Grid"; |
| stat_lead_fraction | float (time=1, yc=432, xc=432); |
| | :coverage_content_type = "qualityInformation"; |
| | long_name = "lead waveform detections per valid waveforms in grid cell"; |
| | coordinates = "time lat lon"; |
| | grid_mapping = "Lambert_Azimuthal_Grid"; |
| | units = "1"; |
| stat_n_total_waveforms | float (time=1, yc=432, xc=432); |
| | :coverage_content_type = "qualityInformation"; |
| | coordinates = "time lat lon"; |
| | grid_mapping = "Lambert_Azimuthal_Grid"; |
| | long_name = "number of total measurements per grid cell"; |
| | units = "1"; |
| | float (time=1, yc=432, xc=432); |
| stat_n_valid_waveforms | float (time=1, yc=432, xc=432); |
| | :coverage_content_type = "qualityInformation"; |
| | grid_mapping = "Lambert_Azimuthal_Grid"; |
| | long_name = "number of valid measurements per grid cell"; |
| | units = "1"; |
| | comment = "definition of valid: either lead or ice"; |
| | coordinates = "time lat lon"; |
| stat_negative_thickness_fraction | float (time=1, yc=432, xc=432); |
| | :coverage_content_type = "qualityInformation"; |
| | coordinates = "time lat lon"; |
| | grid_mapping = "Lambert_Azimuthal_Grid"; |
| | long_name = "fraction of negative sea-ice thickness values"; |
| | units = "1"; |
| | valid_max = 1.0f; // float |
| | valid_min = 0.0f; // float |
| stat_radar_mode | Int (time=1, yc=432, xc=432); |
| | :coverage_content_type = "referenceInformation"; |
| | comment = "median of radar mode flags within grid cells"; |
| | coordinates = "time lat lon"; |
| | flag_meanings ="pulse_limited_lrm doppler_delay_sar doppler_delay_sar_interferometric"; |
| | flag_values = 0B, 1B, 2B; |
| | grid_mapping = "Lambert_Azimuthal_Grid"; |
| | long_name = "radar mode flag"; |
| | units = "1"; |

| | valid_max = 2; // int |
|---|---|
| | valid_min = 0; // int |
| stat_temporal_coverage_day_fraction | float (time=1, yc=432, xc=432); |
| | :coverage_content_type = "qualityInformation"; |
| | omment = "This parameter is defined as len(days_with_observations)/number_of_days_in_grid_period"; |
| | coordinates = "time lat lon"; |
| | grid_mapping = "Lambert_Azimuthal_Grid"; |
| | long_name = "fraction of days with sea-ice thickness data coverage in full grid period"; |
| | units = "1"; |
| stat_temporal_coverage_period_fraction | float (time=1, yc=432, xc=432); |
| | :coverage_content_type = "qualityInformation"; |
| | comment = "This parameter describes the fraction of the period between the first and the last day with observations (irrespectively if all days between first and last day have data coverage): (last_day-first_day)/number_of_days_in_grid_period"; |
| | coordinates = "time lat lon"; |
| | grid_mapping = "Lambert_Azimuthal_Grid"; |
| | long_name = "fraction of daily sea-ice thickness data coverage from first to last day relative to full grid period"; |
| | units = "1"; |
| | valid_max = 1.0f; // float |
| | valid_min = 0.0f; // float |
| stat_temporal_coverage_uniformity_factor | float (time=1, yc=432, xc=432); |
| | :coverage_content_type = "qualityInformation"; |
| | comment = "The uniformity factor indicates if the observation are uniform distributed throughout the period of the grid, e.g. whether all days in the period contribute equally to the full grid period. The values for this parameter range between close to 0 (singular distribution) and 1 (uniform distribution). The factor is computed with by Kolmogorov-Smirnov (KS) test that evaluates the list of days against a uniform distribution (1-D with D being the result of KS test)"; |
| | coordinates = "time lat lon"; |
| | grid_mapping = "Lambert_Azimuthal_Grid"; |
| | long_name = "uniformity of daily sea-ice thickness data coverage in full grid period"; |
| | units = "1"; |
| | valid_max = 1.0f; // float |
| | valid_min = 0.0f; // float |
| stat_temporal_coverage_weighted_center | float (time=1, yc=432, xc=432); |
| | :coverage_content_type = "qualityInformation"; |
| | comment = "This parameter describes the temporal center of the days with observations with taken the number observations on indiviual days into account: mean(day number for all observations)/number_of_days_in_grid_period. A value smaller or larger than 0.5 indicates a possible phase bias."; |
| | coordinates = "time lat lon"; |
| | grid_mapping = "Lambert_Azimuthal_Grid"; |

| | |
|---|---|
| | long_name = "weighted center of sea-ice thickness data coverage within full grid period"; |
| | units = "1"; |
| | valid_max = 1.0f; // float |
| | valid_min = 0.0f; // float |
| stat_valid_fraction | float (time=1, yc=432, xc=432); |
| | :coverage_content_type = "qualityInformation"; |
| | long_name = "fraction of valid to total waveforms"; |
| | units = "1"; |
| | coordinates = "time lat lon"; |
| | grid_mapping = "Lambert_Azimuthal_Grid"; |
| | comment = "definition of valid: either lead or ice"; |

### 7.2.2.5   Flags

| Variable | Attributes |
|---|---|
| region_code | int(time=1, yc=432, xc=432); |
| | :coverage_content_type = "referenceInformation"; |
| | comment = "Added flag for Baltic Sea (flag value 16)"; |
| | coordinates = "time lat lon"; |
| | :flag_values = 0, 1, 2, 3, 4, 5, 6, 7, 8, 9, 10, 11, 12, 13, 14, 15, 16, 20, 21; |
| | flag_meanings = "inland_sea_and_lakes ice_free_oceans sea_of_okhotsk bering hudson_bay st_john baffin_bay east_greenland_sea barents_sea kara_sea laptev_sea east_siberian_sea chukchi_sea beaufort_sea canadian_islands central_arctic valtic_sea land land_outline"; |
| | flag_values = "0, 1, 2, 3, 4, 5, 6, 7, 8, 9, 10, 11, 12, 13, 14, 15, 16, 20, 21"; |
| | grid_mapping = "Lambert_Azimuthal_Grid"; |
| | long_name = "Region code (adapted from NSIDC region mask)"; |
| | units = "1"; |
| | valid_max = 21; // int |
| | valid_min = 0; // int |
| quality_flag | byte (time=1, yc=432, xc=432); |
| | :coverage_content_type = "qualityInformation"; |
| | coordinates = "time lat lon"; |
| | flag_values = 0B, 1B, 2B, 3B; |
| | flag_meanings = "nominal_quality intermediate_quality low_quality no_data"; |
| | grid_mapping = "Lambert_Azimuthal_Grid"; |
| | long_name = "quality indicator flag for the sea ice thickness retrieval"; |
| | standard_name = "sea_ice_thickness status_flag"; |
| status_flag | byte (time=1, yc=432, xc=432); |
| | :coverage_content_type = "qualityInformation"; |
| | coordinates = "time lat lon"; |
| | flag_values = 0B, 1B, 2B, 3B, 4B, 5B; |
| | flag_meanings = "nominal_retrieval no_data open_ocean satellite_pole_hole land_lake_landice retrieval_failed"; |
| | grid_mapping = "Lambert_Azimuthal_Grid"; |

| | |
|---|---|
| | long_name = "status flag for the sea ice thickness retrieval"; |
| | standard_name = "sea_ice_thickness status_flag"; |
| | valid_max = 5B; // byte |
| | valid_min = 0B; // byte |

### 7.2.2.6  Dimensions

| Variable | Attributes |
|---|---|
| lat | Float |
| | :coverage_content_type = "coordinate"; |
| | units = "degrees north"; |
| | long_name = "latitude coordinate"; |
| | standard_name = "latitude"; |
| | grid_mapping = "Lambert_Azimuthal_Grid"; |
| | coordinates = "xc yc"; |
| lon | Float |
| | :coverage_content_type = "coordinate"; |
| | units = "degrees east"; |
| | long_name = "longitude coordinate"; |
| | standard_name = "longitude"; |
| | grid_mapping = "Lambert_Azimuthal_Grid"; |
| | coordinates = "xc yc"; |
| time | double(time=1); |
| | :coverage_content_type = "coordinate"; |
| | standard_name = "time"; |
| | units = "seconds since 1970-01-01"; |
| | long_name = "reference time of product"; |
| | axis = "T"; |
| | calendar = "standard"; |
| | bounds = "time_bnds"; |
| time_bnds | double (time=1, nv=2); |
| | units = "seconds since 1970-01-01"; |
| Lambert_Azimuthal_Grid | Byte (dimensionless) |
| | false_easting = 0.0; // double |
| | false_northing = 0.0; // double |
| | grid_mapping_name = "lambert_azimuthal_equal_area"; |
| | inverse_flattening = 298.257223563; // double |
| | latitude_of_projection_origin = 90.0; // double |
| | longitude_of_projection_origin = 0.0; // double |
| | proj4_string = "+proj=laea +lon_0=0 +datum=WGS84 +ellps=WGS84 +lat_0=90.0"; |
| | semi_major_axis = 6378137.0; // double |
| xc | double xc(xc=432); |
| | :coverage_content_type = "coordinate"; |
| | standard_name = "projection_x_coordinate"; |
| | long_name = "x coordinate of projection (eastings)"; |
| | units = "km"; |
| yc | double(yc=432); |

| | |
|---|---|
| | `:coverage_content_type = "coordinate";` |
| | `standard_name = "projection_y_coordinate";` |
| | `units = "km";` |
| | `long_name = "y coordinate of projection (eastings)";` |

# 8   Data Access Information

## 8.1   Download

CryoSat-2 data products can be accessed at the public ftp service of the Alfred Wegener Institute without prior registration.

ftp://ftp.awi.de/sea_ice/product/cryosat2/

Due to data size, data access is limited to l2p and l3c products. Products of lower processing levels are made available upon request (see section 8.2.2).

### 8.1.1   Near real-time (NRT) products

Products based on CryoSat-2 near-real time data are not stored for the entire data record on the ftp site but are deleted once the reprocessed data becomes available. NRT products are generated with a delay of 2 days.

| l2p | Link | ftp://ftp.awi.de/sea_ice/product/cryosat2/v2p4/nh/l2p_trajectory/LATEST/ |
|---|---|---|
| | Subfolder | None |
| l3c (weekly) | Link | ftp://ftp.awi.de/sea_ice/product/cryosat2/v2p4/nh/l3c_grid/isoweek/LATEST/ |
| | Subfolder | None |
| l3m (monthly) | Link | ftp://ftp.awi.de/sea_ice/product/cryosat2/v2p4/nh/l3c_grid/month/LATEST/ |
| | Subfolder | None |

### 8.1.2   Reprocessed (REP) products

REP products are generated with a delay of 33 days. Once a REP data file becomes available, it supersedes the corresponding NRT data file.

| l2p | Link | ftp://ftp.awi.de/sea_ice/product/cryosat2/v2p4/nh/l2p_trajectory/ |
|---|---|---|
| | Subfolder | <year>/<month> e.g., 2014/01/ |
| l3c (weekly) | Link | kftp://ftp.awi.de/sea_ice/product/cryosat2/v2p4/nh/l3c_grid/isoweek/ |
| | Subfolder | <year> e.g., 2014/ |
| l3m (monthly) | Link | ftp://ftp.awi.de/sea_ice/product/cryosat2/v2p4/nh/l3c_grid/month/ |
| | Subfolder | <year> e.g., 2014/ |

## 8.2    Visualization

### 8.2.1    netCDF

The NASA Panoply netCDF, HDF and GRIB data viewer (https://www.giss.nasa.gov/tools/panoply/) can be used as an offline viewer and is available for multiple platforms. See Figure 13 for an example.
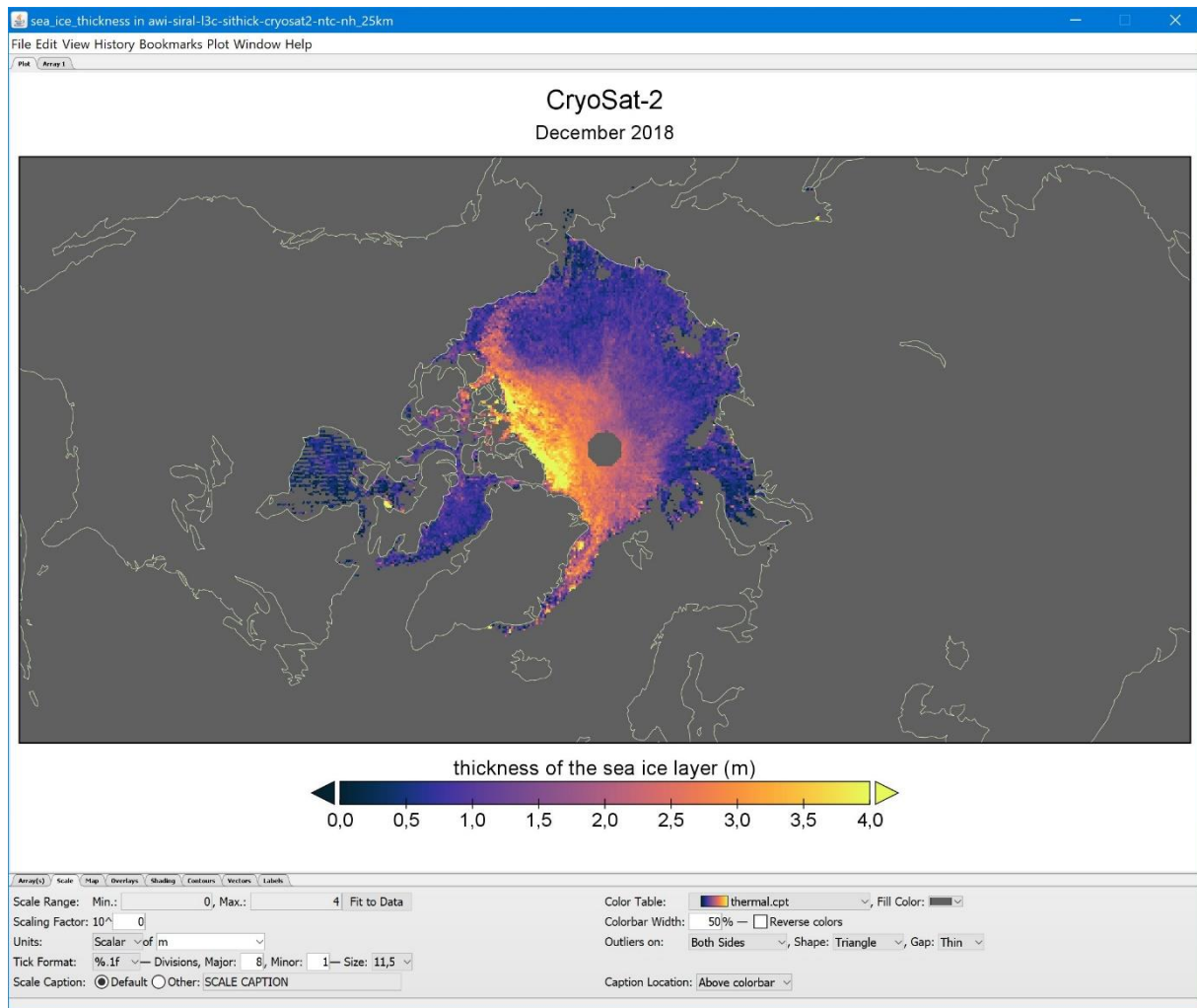


Figure 13: Visualization of a monthly gridded (l3c) sea-ice thickness field with panoply.

### 8.2.2    GeoTiff

Geotiff products can be visualized with any GIS software. Open sources exist, e.g., QGIS (https://qgis.org/).
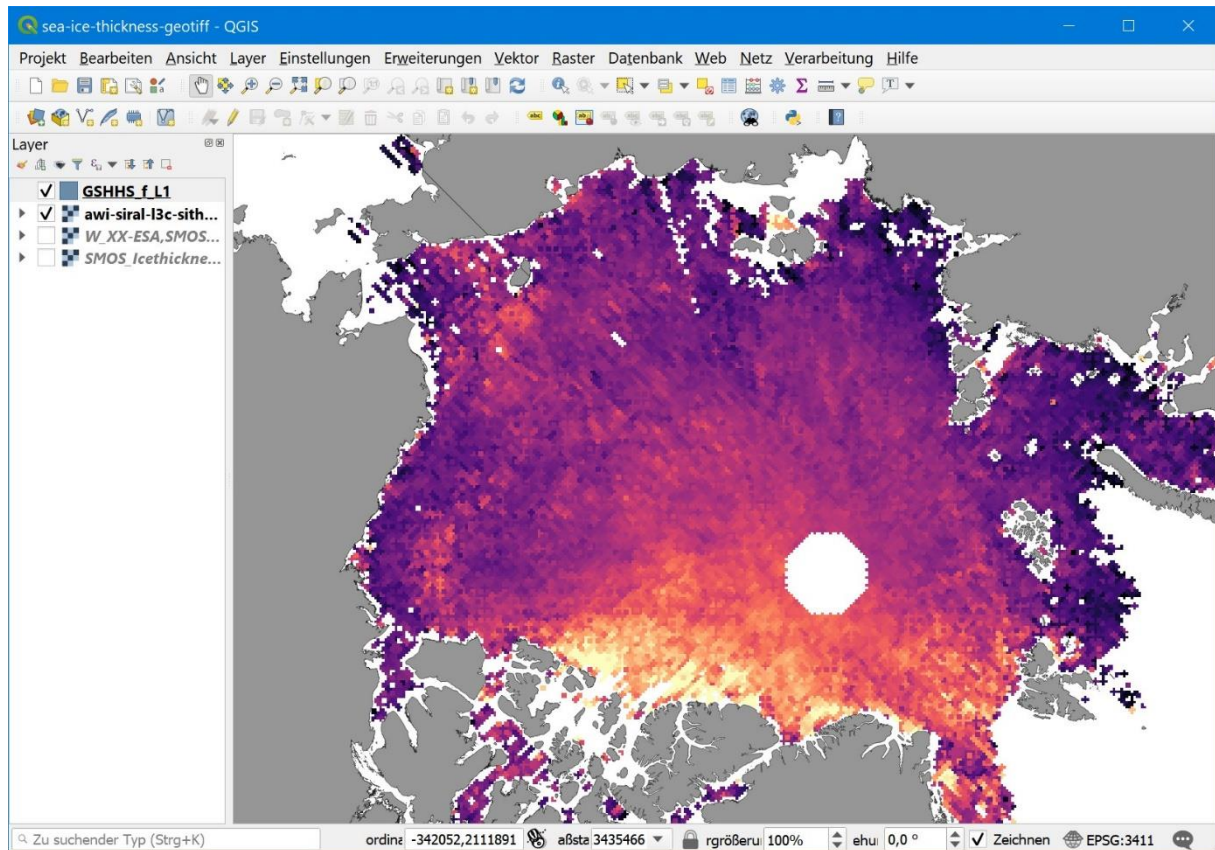
Figure 14: Visualization of sea-ice thickness geotiff file in a geographic information system (GIS)

## 8.3    Point of Contact

For any inquiries please use the email (cs2smos-support@awi.de) or alternatively web contact form of meereisportal.de (https://www.meereisportal.de/en/contact/).

# 9    Known Issues

Various components of the sea-ice thickness algorithm are an active field of research with expected gradual improvements in future versions. Without claim of completeness or order of relevance, these fields of research include:

1. Radar ranging over sea ice surfaces with varying snow depth, stratigraphy, and surface roughness
2. Estimation of instantaneous sea surface height in the marginal ice zone with low wave heights and continuity to open ocean sea surface height observations
3. Estimation of snow depth and density from re-analysis with realistic interannual and decadal variability

These topics affect various aspects of the sea-ice thickness algorithm and improvements will be implemented in future product updates upon availability. This section provides an overview of the known issues and limitations of the current algorithm and auxiliary data sets.

## 9.1    Freeboard

### 9.1.1    Snow backscatter

A key assumption in the ranging algorithm over snow covered sea ice is that the main scattering horizon is the ice/snow interface for Arctic sea ice conditions between October and April. There is however ample evidence in the scientific literature that backscatter from the snow layer can have an effect on radar ranging with Ku-Band frequencies (e.g., Kurtz et al., 2014; Kwok R., 2014; Ricker et al., 2015; Nandan et al., 2017).

Snow backscatter causes the freeboard to be biased high and thus leads to an overestimation of sea ice thickness. The ranging algorithm used for the AWI sea ice thickness product is empirical without snow depth as an input parameter, however the geometric correction used for converting the radar-derived freeboard into sea ice freeboard depends on snow depth and is an obvious candidate for including snow backscatter related range biases. However, little is known over the temporal and spatial variability of this effect on basin scale.

### 9.1.2    Surface Roughness

It has been shown that the magnitude of surface roughness as well as its distribution function (Landy et al. 2018) has an impact on the leading edge of the waveform. The surface roughness, respectively the leading-edge width will impact the radar range and thus freeboard, especially with a fixed TFMRA threshold. An improved handling of surface roughness in the freeboard retrieval is under investigation

## 9.2    Sea Ice Thickness

### 9.2.1    Snow depth on sea ice

The current use of a static monthly snow climatology on Arctic Sea Ice (from in-situ observation and satellite data) with a resolution of 25km does not properly capture the interannual and decadal variability of snow depth and density, even with a scaling for first-year sea ice. In addition, the information does not represent variations on footprint scale. This specifically impact the thickness of young sea ice, which might have only a thin snow layer but will always be assigned the full climatological snow depth in the processing.

### 9.2.2    Sea-Ice Density

Like snow depth, the density values for sea ice also depend on a sparse set of observations and may not describe the actual density variations at the scales radar footprint resolution. The observational database originates on samples from sea ice cores, which show a significant parameter range (see e.g. Alexandrov et al. 2010).

The actual sea ice density on larger scales both depends on small-scale porosity, brine volume and the large-scale porosity of deformed & blocky sea ice. We assume that especially the variation driven by deformation are not well represented by the density samples of sea ice cores.

First results from airborne surveys with coincident observations of sea-ice thickness, freeboard, and snow depth (Jutila et al., 2021) indicate discrepancies between the climatological sea ice density used in the CryoSat-2 processing chain and observed values. The largest difference has been found for multi-year sea ice, where the airborne data suggest a value of 902.4 kg/m$^3$, compared to 882.0 kg/m$^3$ of the Alexandrov climatology. For first year sea ice the airborne data also indicates a higher mean value of 925.4 kg/m$^3$ that the climatology (916.7 kg/m$^3$).

Using higher ice density values has the effect of proportionally increased sea ice thickness. Internal validation and product quality control however does not show that the AWI CryoSat-2 thicknesses are biased low. The introduction of more realistic sea ice densities in the processor must therefore be coupled to improvements in the radar freeboard retrieval and snow mass auxiliary data. This task will be addressed in future versions of the AWI CryoSat-2 sea ice product.

# 10  References

Alexandrov, V., Sandven, S., Wahlin, J., and Johannessen, O. M. (2010). The relation between sea ice thickness and freeboard in the arctic. The Cryosphere, 4:373–380.

Jutila, A., Hendricks, S., Ricker, R., von Albedyll, L., Krumpen, T., and Haas, C.: Retrieval and parametrisation of sea-ice bulk density from airborne multi-sensor measurements, The Cryosphere Discuss. [preprint], https://doi.org/10.5194/tc-2021-149, in review, 2021.

Kurtz, N. T., Galin, N., and Studinger, M.: An improved CryoSat-2 sea ice freeboard retrieval algorithm through the use of waveform fitting, The Cryosphere, 8, 1217-1237, https://doi.org/10.5194/tc-8-1217-2014, 2014.

Kwok, R. and G. F. Cunningham (2015). Variability of Arctic sea ice thickness and volume from CryoSat-2.", Philosophical Transactions of the Royal Society a-Mathematical Physical and Engineering Sciences 373(2045).

Landy J. C., M. Tsamados and R. K. Scharien, "A Facet-Based Numerical Model for Simulating SAR Altimeter Echoes From Heterogeneous Sea Ice Surfaces," in IEEE Transactions on Geoscience and Remote Sensing. doi: 10.1109/TGRS.2018.2889763

Nandan, V., Geldsetzer, T., Yackel, J., Mahmud, M., Scharien, R., Howell, S., King J., Ricker R., Else, B. (2017). Effect of snow salinity on CryoSat-2 Arctic first-year sea ice freeboard measurements. Geophysical Research Letters, 44, 10,419– 10,426. https://doi.org/10.1002/2017GL074506

Mallett, R. D. C., Lawrence, I. R., Stroeve, J. C., Landy, J. C., and Tsamados, M.: Brief communication: Conventional assumptions involving the speed of radar waves in snow introduce systematic underestimates to sea ice thickness and seasonal growth rate estimates, The Cryosphere, 14, 251–260, https://doi.org/10.5194/tc-14-251-2020, 2020.

Paul, S., Hendricks, S., Ricker, R., Kern, S., and Rinne, E.: Empirical parametrization of Envisat freeboard retrieval of Arctic and Antarctic sea ice based on CryoSat-2: progress in the ESA Climate Change Initiative, The Cryosphere, 12, 2437-2460, https://doi.org/10.5194/tc-12-2437-2018, 2018.

Ricker, R., Hendricks, S., Helm, V. , Skourup, H. and Davidson, M. (2014): Sensitivity of CryoSat-2 Arctic sea-ice freeboard and thickness on radar-waveform interpretation, The Cryosphere, 8 (4), pp. 1607-1622. doi: 10.5194/tc-8-1607-2014

Ricker, R., Hendricks, S. , Perovich, D. K. , Helm, V. and Gerdes, R. (2015): Impact of snow accumulation on CryoSat-2 range retrievals over Arctic sea ice: An observational approach with buoy data, Geophysical Research Letters, 42 (11), pp. 4447-4455 . doi: 10.1002/2015GL064081

Warren, S.; Rigor, I.; Untersteiner, N.; Radionov, V.; Bryazgin, N.; Aleksandrov, V. & Colony, R., Snow depth on Arctic sea ice, *Journal of Climate,* 1999*, 12*, 1814-1829